

# Technical Report

## Rockburst Model Validation

Approved for public release; distribution is unlimited

March 2004



Prepared for:  
Defense Threat Reduction Agency  
8725 John J. Kingman Road, MS-6201  
Fort Belvoir, VA 22060-6201

DSWA01-97-C-0124

Kenneth F. Sprenke  
Allan C. Rohay  
Michael C. Stickney

Prepared by:

University of Idaho  
Department of Geological Sciences  
P.O. Box 443022  
Moscow, ID 83844-3022

20040604 149

DESTRUCTION NOTICE:

Destroy this report when it is no longer needed.  
Do not return to sender.

PLEASE NOTIFY THE DEFENSE THREAT REDUCTION  
AGENCY, ATTN: BDMI, 8725 JOHN J. KINGMAN ROAD,  
MS-6201, FT BELVOIR, VA 22060-6201, IF YOUR ADDRESS  
IS INCORRECT, IF YOU WISH IT DELETED FROM THE  
DISTRIBUTION LIST, OR IF THE ADDRESSEE IS NO  
LONGER EMPLOYED BY YOUR ORGANIZATION.

## DISTRIBUTION LIST UPDATE

This mailer is provided to enable DTRA to maintain current distribution lists for reports. (We would appreciate you providing the requested information.)

- ☐ Add the individual listed to your distribution list.
- ☐ Delete the cited organization/individual.
- ☐ Change of address.

**Note:**

Please return the mailing label from the document so that any additions, changes, corrections or deletions can be made easily. For distribution cancellation or more information call DTRA/BDMI (703) 767-4724.

NAME: \_\_\_\_\_

ORGANIZATION: \_\_\_\_\_

**OLD ADDRESS**

**NEW ADDRESS**

\_\_\_\_\_  
\_\_\_\_\_  
\_\_\_\_\_

\_\_\_\_\_  
\_\_\_\_\_  
\_\_\_\_\_

TELEPHONE NUMBER: (    ) \_\_\_\_\_

**DTRA PUBLICATION NUMBER/TITLE**

**CHANGES/DELETIONS/ADDITONS, etc.**  
*(Attach Sheet if more Space is Required)*

\_\_\_\_\_  
\_\_\_\_\_  
\_\_\_\_\_

\_\_\_\_\_  
\_\_\_\_\_  
\_\_\_\_\_

DTRA or other GOVERNMENT CONTRACT NUMBER: \_\_\_\_\_

CERTIFICATION of NEED-TO-KNOW BY GOVERNMENT SPONSOR (if other than DTRA):

SPONSORING ORGANIZATION: \_\_\_\_\_

CONTRACTING OFFICER or REPRESENTATIVE: \_\_\_\_\_

SIGNATURE: \_\_\_\_\_

DEFENSE THREAT REDUCTION AGENCY  
ATTN: BDMI  
8725 John J. Kingman Road, MS-6201  
Ft Belvoir, VA 22060-6201

DEFENSE THREAT REDUCTION AGENCY  
ATTN: BDMI  
8725 John J. Kingman Road, MS-6201  
Ft Belvoir, VA 22060-6201

REPORT DOCUMENTATION PAGE			Form Approved	
Public reporting burden for this collection of information is estimated to average 1 hour per response, including the time for reviewing instructions, searching existing data sources, gathering and maintaining the data needed, and completing and reviewing the collection of information. Send comments regarding this burden, estimate or any other aspect of this collection of information, including suggestions for reducing this burden, to Washington Headquarters Services, Directorate for Information Operations and Reports, 1215 Jefferson Davis Highway, Suite 1204, Arlington, VA 22202-4302, and to the Office of Management and Budget, Paperwork Reduction Project (0704-0188), Washington, DC 20503.				
1. AGENCY USE ONLY (Leave blank)		2. REPORT DATE March 2004		3. REPORT TYPE AND DATES COVERED Technical 971001-000930
4. TITLE AND SUBTITLE  Rockburst Model Validation			5. FUNDING NUMBERS  C - DSWA01-97-C-0124 PE - CD PR - CD TA - N/A WU - DH649370	
6. AUTHOR(S)  Kenneth F. Sprenke, Alan C. Rohay, and Michael C. Stickney				
7. PERFORMING ORGANIZATION NAME(S) AND ADDRESS(ES)  University of Idaho Department of Geological Sciences P.O. Box 443022 Moscow, ID 83844-3022			8. PERFORMING ORGANIZATION REPORT NUMBER	
9. SPONSORING/MONITORING AGENCY NAME(S) AND ADDRESS(ES)  Defense Threat Reduction Agency 8725 John J. Kingman Road, MS-6201 Fort Belvoir, VA 22060-6201  TDOS/Jerrett			10. SPONSORING/MONITORING AGENCY REPORT NUMBER  DTRA-TR-00-15	
11. SUPPLEMENTARY NOTES  This work was sponsored by the Defense Threat Reduction Agency under RDT&E RMC Code B 4613 D CD CD 64938 5P50 A 25904D.				
12a. DISTRIBUTION/AVAILABILITY STATEMENT  Approved for public release, distribution unlimited.			12b. DISTRIBUTION CODE	
13. ABSTRACT (Maximum 200 words)  Characterization of mining-related seismic events is critical to the implementation of the Comprehensive Nuclear Test-Ban Treaty monitoring system. Mine seismicity from uncontrolled sources are particularly troublesome, with magnitudes up to 4 or 5, producing signal strengths comparable to 1-10 kiloton contained nuclear explosions. The Coeur d'Alene district in northern Idaho is the most rockburst-prone mining district in the United States, producing a daily average of about 3 events with magnitudes ranging from 0 to 4. The hypocenter of many of these events are determined to an accuracy of within 30 meters by in-mine rockburst monitoring systems operated by the mining companies. Focal mechanism studies based on these systems, and a district-wide surface seismic network, indicate predominantly dilatational first motions events. We deployed a local seismograph system in the summer of 1998 to determine the source parameters and moment tensors for seismic events in the region in particular to confirm the shear implosional mechanisms suggested by the first motion studies. In this study, ground motions from four surface stations and one underground station were inverted to determine the complete moment tensor of a relatively large rockburst in the Coeur d'Alene Mining District in northern Idaho. Many rockbursts induced by the mining process show shear implosional source mechanisms a feature that should be useful to discriminate mining-related events from underground explosions.				
14. SUBJECT TERMS Rockbursts   Mining-related   Seismicity   Implosions   Underground Explosions			15. NUMBER OF PAGES  60	
17. SECURITY CLASSIFICATION OF REPORT UNCLASSIFIED			16. PRICE CODE	
18. SECURITY CLASSIFICATION OF THIS PAGE UNCLASSIFIED		19. SECURITY CLASSIFICATION OF ABSTRACT UNCLASSIFIED		20. LIMITATION OF ABSTRACT SAR

CLASSIFIED BY:  
N/A since Unclassified

DECLASSIFY ON:  
N/A since Unclassified

7. PERFORMING ORGANIZATION NAMES (S) (Continued):

Battelle Memorial Institute  
Pacific Northwest Division  
Richland, VA 99352

Montana Bureau of Mines and Geology  
Earthquake Studies Office  
Butte, MT 59701

## Summary

Unlike typical earthquakes, rockbursts and mine collapses often have regional waveforms that may be confused with nuclear explosions. Such seismic signals could present false alarms to organizations tasked with verifying a Comprehensive Test Ban Treaty. Mines may also provide potential locations for evasion, through partial decoupling or triggered shear failure. The Coeur d'Alene district in northern Idaho is the most rockburst-prone mining district in the United States, producing a daily average of about 3 events with magnitudes ranging from 0 to 4. The hypocenter locations of many of these events are determined to an accuracy of within 30 meters by in-mine rockburst monitoring systems operated by the mining companies. The largest and most frequent events are located near an area of active mining at a depth of 1650 meters at one of three producing mines. Focal mechanism studies based on these systems, and a district-wide surface seismic network, indicate dominantly dilatational first motion events. We deployed a local seismic system in the summer of 1998 to determine the source parameters and moment tensors for seismic events in the region, in particular to confirm the shear implosional mechanisms suggested by the first-motion studies.

Characterization of mining-related seismic events is critical to the implementation of the Comprehensive Nuclear Test-Ban Treaty monitoring system. Mine seismicity from uncontrolled sources are particularly troublesome, with magnitudes up to 4 or 5, producing signal strengths comparable to 1-10 kiloton contained nuclear explosions. In this study, ground motions from four surface stations and one underground station were inverted to determine the complete moment tensor of a relatively large rock burst in the Coeur d'Alene Mining District in northern Idaho. Many rock bursts, induced by the mining process, show shear implosional source mechanisms, a feature that should be useful to discriminate mining-related events from underground explosions.

# CONVERSION TABLE

Conversion Factors for U.S. Customary to metric (SI) units of measurement.

MULTIPLY  $\xrightarrow{\hspace{1cm}}$  BY  $\xrightarrow{\hspace{1cm}}$  TO GET  
TO GET  $\xleftarrow{\hspace{1cm}}$  BY  $\xleftarrow{\hspace{1cm}}$  DIVIDE

angstrom	1.000 000 x E -10	meters (m)
atmosphere (normal)	1.013 25 x E +2	kilo pascal (kPa)
bar	1.000 000 x E +2	kilo pascal (kPa)
barn	1.000 000 x E -28	meter <sup>2</sup> (m <sup>2</sup> )
British thermal unit (thermochemical)	1.054 350 x E +3	joule (J)
calorie (thermochemical)	4.184 000	joule (J)
cal (thermochemical/cm <sup>2</sup> )	4.184 000 x E -2	mega joule/m <sup>2</sup> (MJ/m <sup>2</sup> )
curie	3.700 000 x E +1	*giga bacquerel (GBq)
degree (angle)	1.745 329 x E -2	radian (rad)
degree Fahrenheit	$t_K = (t^{\circ}F + 459.67)/1.8$	degree kelvin (K)
electron volt	1.602 19 x E -19	joule (J)
erg	1.000 000 x E -7	joule (J)
erg/second	1.000 000 x E -7	watt (W)
foot	3.048 000 x E -1	meter (m)
foot-pound-force	1.355 818	joule (J)
gallon (U.S. liquid)	3.785 412 x E -3	meter <sup>3</sup> (m <sup>3</sup> )
inch	2.540 000 x E -2	meter (m)
jerk	1.000 000 x E +9	joule (J)
joule/kilogram (J/kg) radiation dose absorbed	1.000 000	Gray (Gy)
kilotons	4.183	terajoules
kip (1000 lbf)	4.448 222 x E +3	newton (N)
kip/inch <sup>2</sup> (ksi)	6.894 757 x E +3	kilo pascal (kPa)
ktap	1.000 000 x E +2	newton-second/m <sup>2</sup> (N-s/m <sup>2</sup> )
micron	1.000 000 x E -6	meter (m)
mil	2.540 000 x E -5	meter (m)
mile (international)	1.609 344 x E +3	meter (m)
ounce	2.834 952 x E -2	kilogram (kg)
pound-force (lbs avoirdupois)	4.448 222	newton (N)
pound-force inch	1.129 848 x E -1	newton-meter (N-m)
pound-force/inch	1.751 268 x E +2	newton/meter (N/m)
pound-force/foot <sup>2</sup>	4.788 026 x E -2	kilo pascal (kPa)
pound-force/inch <sup>2</sup> (psi)	6.894 757	kilo pascal (kPa)
pound-mass (lbm avoirdupois)	4.535 924 x E -1	kilogram (kg)
pound-mass-foot <sup>2</sup> (moment of inertia)	4.214 011 x E -2	kilogram-meter <sup>2</sup> (kg-m <sup>2</sup> )
pound-mass/foot <sup>3</sup>	1.601 846 x E +1	kilogram-meter <sup>3</sup> (kg/m <sup>3</sup> )
rad (radiation dose absorbed)	1.000 000 x E -2	**Gray (Gy)
roentgen	2.579 760 x E -4	coulomb/kilogram (C/kg)
shake	1.000 000 x E -8	second (s)
slug	1.459 390 x E +1	kilogram (kg)
torr (mm Hg, 0° C)	1.333 22 x E -1	kilo pascal (kPa)

\*The bacquerel (Bq) is the SI unit of radioactivity; 1 Bq = 1 event/s.

\*\*The Gray (GY) is the SI unit of absorbed radiation.



# Table of Contents

Section	Page
SUMMARY .....	iii
CONVERSION TABLE .....	iv
FIGURES .....	vi
TABLES.....	vii
 1 DEPLOYMENT OF A LOCAL NETWORK AND SEISMIC DATA COLLECTION OF NORTHERN IDAHO ROCKBURSTS.....	     1
1.1 SUMMARY STATEMENT .....	1
1.2 INTRODUCTION.....	1
1.3 PREVIOUS WORK IN THE COEUR D'ALENE DISTRICT .....	3
1.4 OBJECTIVES .....	8
1.5 SEISMIC DATA FROM SENSOR NETWORK AND FROM IN-MINE STATIONS.....	 11
1.6 DATA FROM SOURCES AT REGIONAL DISTANCES .....	13
 2 SEISMIC SOURCE PARAMETERS OF ROCK BURSTS COEUR D'ALENE MINING DISTRICT, IDAHO .....	   16
2.1 INTRODUCTION.....	16
2.2 OBJECTIVE.....	16
2.3 SEISMIC MOMENT .....	18
2.4 MOMENT MAGNITUDE.....	19
2.5 P-WAVE AND S-WAVE ENERGY .....	19
2.6 RADIATION EFFICIENCY.....	19
2.7 SOURCE DIMENSIONS.....	20
2.8 PULSE DURATION AND RUPTURE VELOCITY .....	20
2.9 STRESS DROP .....	21
2.10 APPARENT STRESS .....	21
2.11 DYNAMIC STRESS DROP .....	21
2.12 FAULT DISPLACEMENT.....	21
2.13 FAULT PLANE SOLUTIONS-MOMENT TENSOR INVERSION .....	22
2.14 ANALYSIS OF NEAR-FIELD DATA.....	26
2.15 A TEMPLATE FOR SHEAR-IMPLOSIONAL ROCKBURSTS.....	38
 3 REFERENCES.....	 41
 DISTRIBUTION LIST .....	 DL-1

## Figures

Figure		Page
1	Location Map of Mines in the Coeur d'Alene Mining District of Northern Idaho.....	2
2	Travel time curve for seismic events in the Coeur d'Alene district based on independently known hypocentral locations.....	3
3	Longitudinal section view of the Lucky Friday Mine showing rockburst hypocenters.....	4
4	Fault plane solutions for events below the 5400 sub-level of the Lucky Friday Mine.....	5
5	Concentration contours for the P, I, and T axes plotted on equal area stereonet.....	6
6	Vertical Waveforms from Rockbursts Associated with Blasting at the Lucky Friday Mine...	8
7	Displacement Amplitude Spectra of 26 signals with dilational first motions.....	12
8	Waveforms recorded at the Yellowknife Array, 1500 km north of the Lucky Friday Mine...	12
9	Location of stations and epicenters of largest rockbursts recorded.....	16
10	Displacements recorded at MOR.....	17
11	The average day at the Lucky Friday Mine. Although most events occur at blasting times, events can occur at any time of day.....	22
12	Greens functions for the study area. The simulated M3.1 hypocenter is at a depth of 1750 m in the center of the main area. The accelerometer stations are indicated.....	24
13	The nine couples composing the seismic moment tensor.....	25
14	Displacement amplitudes at ATL for the largest burst recorded in this study. The P and S picks are also shown. See Figure 9 for locations of the stations.....	26
15	Displacement amplitudes at DED for the largest burst recorded in this study. The P and S picks are also shown. See Figure 9 for locations of the stations.....	27
16	Displacement amplitudes at MOR for the largest burst recorded in this study. The P and S picks are also shown. See Figure 9 for locations of the stations.....	28
17	Displacement amplitudes at GOL for the largest burst recorded in this study. The P and S picks are also shown. See Figure 9 for locations of the stations.....	29
18	Displacement amplitudes at MIL for the largest burst recorded in this study. The P and S picks are also shown. See Figure 9 for locations of the stations.....	30
19	The P displacements for the largest burst observed the shown on a plan view of the mine area. The implosional (negative M33) nature of the event is clearly evident.....	31

## Figures (Cont.)

Figure	Page
20 The P displacement polarity plotted on the lower hemisphere of an equal-area stereographic projection .....	32
21 The SV displacements for the largest burst observed shown on a plan view of the mine area. The shear (negative M13) nature of the event is evident.....	33
22 The SH displacements for the largest burst observed shown on a plan view of the mine area. The shear (negative M13) nature of the event is apparent.....	34
23 Waveforms at CSN seismic station WALA from a 3.6 mine tremor on Feb. 9, 1996 (upper) and from a recent northern Idaho earthquake (lower). Approximate group velocities of 7.8, 6.1 and 3.7 km/s are shown.....	38
24 Waveforms recorded at regional distances for the largest burst observed during this study .....	39

## Tables

Table		Page
1	Event Catalog from the CNSS.....	9
2	Event Catalog from the In-Mine System.....	9
3	Blast Times for Mines in the Coeur d'Alene. ....	11
4	Mine Coordinates. ....	11
5	Regional Rockburst Catalog (1982-1999).....	14

## SECTION 1

### DEPLOYMENT OF A LOCAL NETWORK AND SEISMIC DATA COLLECTION OF NORTHERN IDAHO ROCKBURSTS

#### 1.1 Summary Statement.

Unlike typical earthquakes, rockbursts and mine collapses often have regional waveforms that may be confused with nuclear explosions. Such seismic signals could present false alarms to organizations tasked with verifying a Comprehensive Test Ban Treaty. Mines may also provide potential locations for evasion, through partial decoupling or triggered shear failure. The Coeur d'Alene district in northern Idaho is the most rockburst-prone mining district in the United States, producing a daily average of about 3 events with magnitudes ranging from 0 to 4. The hypocenter locations of many of these events are determined to an accuracy of within 30 meters by in-mine rockburst monitoring systems operated by the mining companies. The largest and most frequent events are located near an area of active mining at a depth of 1650 meters at one of three producing mines. Focal mechanism studies based on these systems, and a district-wide surface seismic network, indicate dominantly dilatational first motion events. We deployed a local seismic system in the summer of 1998 to determine the source parameters and moment tensors for seismic events in the region, in particular to confirm the shear implosional mechanisms suggested by the first-motion studies.

#### 1.2 Introduction.

Rockbursts are seismic events that cause visible damage to underground excavations. Rockbursts are major hazards in mines worldwide, particularly in Canada and South Africa, where they cause production delays, losses of millions of dollars per year, in addition to injuries and death to miners. Additionally, Heuze (1994) pointed out the potential to use these events to camouflage nuclear tests. Considerably more study is needed to characterize systematic differences between mine tremors and other seismic sources. Mine explosions and rockbursts are similar in some ways to natural earthquakes in that they are often related to shear failures on fault planes in a rockmass (McGarr, 1984; McGarr, 1971; Spottiswoode and McGarr, 1975; McGarr et al., 1979). However, results from focal mechanism studies of mining events indicate that alternative mechanisms other than simple shear failure are common.

Simple explanations exist for the deviation of the moment tensor solutions from double-couple solutions, including curved failure planes, incorrect hypocenter depths, and multiple ruptures. However, in the case of mining events, a volumetric component seems to be common, as is indicated by a preponderance of dilatational P wave arrivals (Williams and Arabasz, 1989; Wong et al., 1989; Stickney and Sprenke, 1993). Shear implosional models for mining events have been proposed by Teisseyre (1980), and Rudej and Sileny (1985). At the other extreme, shear-tensional models for mine events have also been proposed (Teisseyre, 1980; Gibowicz and Kijko, 1994).

The failure mechanisms associated with mining-related seismic events in the Coeur d'Alene mining district of northern Idaho are uncertain. Problems associated with rockbursting cause accidents and increase the cost of mining. The first step toward mitigating rockburst hazards is a fundamental understanding of their cause. Prior to 1980, rockbursts in the district were attributed to the failure of pillars ahead of advancing mine faces; during the 1980s however, it became apparent from observations of in-mine damage that shear slip along faults and bedding planes was also a source of rockbursts (Blake, 1984; Blake and Cuvelier, 1990). Several rigorous studies of mine tremors in deep South African gold mines suggest that natural earthquakes and mining-related seismic events share a similar focal mechanism: pure shear failure (McGarr, 1971, 1984; McGarr et al., 1975; Spottiswoode and McGarr,

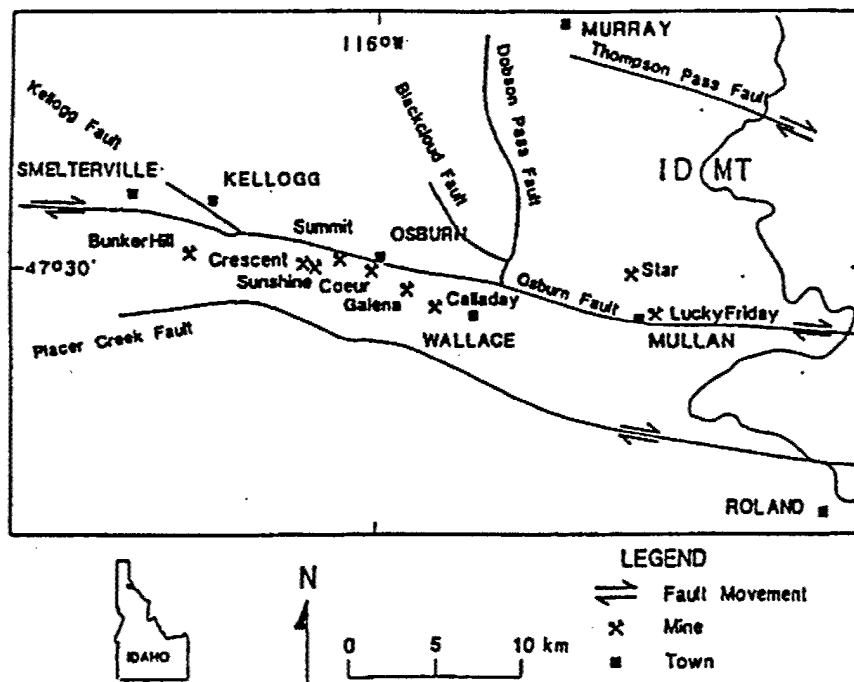


Figure 1. Location Map of Mines in the Coeur d'Alene Mining District of Northern Idaho.

1975). However, the presence of void space near mine-related foci theoretically also allows for a compressive "implosional" component of stress release (Teisseyre, 1980; Stiller et al., 1983; Kozak and Sileny, 1985; Rudajev and Sileny, 1985). Many researchers have reported a preponderance of dilatational first motions associated with mining-related seismic events: in South African gold mines (Gane et al., 1952; etc.), and in coal mines worldwide (See Wong and McGarr (1990) and Wong et al. (1989) for reviews). However, in a review of the focal sphere coverage of these observations, Wong and McGarr (1990) could find only five cases of implosional failure that were worthy of consideration and they discredited four of these five cases on the bases of inadequate focal sphere coverage or inaccurate hypocenter locations. They also found insufficient evidence to validate a shear-implosional model for coal mine slip events.

Rockbursts and mine collapses are often observed to have regional waveforms that are unlike typical earthquakes and which can be confused with nuclear explosions (Taylor, 1994, Bennett et al., 1995, Bennett et al., 1996). Mining-induced events cannot be discriminated on the basis of hypocentral depth. The relatively low excitation of Love and Rayleigh waves tend to make mining-induced events, especially those with a large implosional component to the moment tensor, appear similar to explosions when using classical  $M_s$  vs.  $m_b$  discriminants. Bennett et al., (1995, 1996) indicate that the  $S/P$  or  $L_g/P$  ratios for mining-induced events around the globe are larger than observed for nuclear explosions, which makes the regional signals appear more similar to typical earthquakes. Conversely, Taylor (1994) observed a mining-related event in Utah that had a low  $L_g/P_g$  ratio, and other signal characteristics including a lack of Love waves, that caused this event to be classified as an explosion in an extensive discrimination study in the western U.S. (Taylor, 1991). Pechman et al. (1995) note that a mine collapse in southeastern Wyoming also had  $m_b$ - $M_w$  and  $M_L$ - $M_w$  differences that were more typical of nuclear explosions, and also noted the lack of  $P_n$  and Love waves, also noted to be a feature of nuclear explosion waveforms.

### 1.3 Previous Work in the Coeur d'Alene District.

The Coeur d'Alene mining district, one of the largest lead-, zinc-, silver-producing areas of the world, lies along the Osburn fault in northern Idaho near the Montana border (Figure 1). The tectonic setting of the district within the larger Lewis and Clark Zone has been described by Hobbs et al. (1965); Wallace et al. (1990); and Stickney and Bartholomew (1987). Although seismicity in the district has historically been related to mining activity, tectonic events also occur (Sprenke et al., 1991; Sprenke and Stickney, 1993; Breckenridge, Sprenke, and Stickney, 1995). To gather more information on the source mechanisms of mining-related seismic events in the Coeur d'Alene district, a district-wide seismograph network was operated using portable instruments for one week during September 1990 (Stickney and Sprenke, 1993), and a district-wide network using up to 28 stations from 1992-1994 (Jung et al., 1994). As a result of these studies, we have observational evidence that dilatational first motions are prevalent in this deep metal-mining district, probably the result of implosional and shear-implosional source mechanisms involving mine openings.

Using data from the district-wide networks, hypocenter locations determined by the in-mine systems, were used to construct a travel time curve (Figure 2) for the district using impulsive body wave travel times for 19 Lucky Friday Mine and two Galena Mine events. The results indicate a half space velocity model with a P wave velocity of  $5.74 \pm 0.02$  km/s and a uniform S wave velocity of  $3.47 \pm 0.05$  km/s (Stickney and Sprenke, 1993).

The preferred modes of failure for the shear events in the district are (1) right-lateral strike-slip movement along steeply dipping northwest striking planes, (2) normal faulting along moderate dipping northerly striking planes, and (3) thrust faulting along randomly striking, shallow dipping planes. P and T axes derived from the fault plane solutions are consistent with the directions of principal horizontal stresses from previous in situ measurements (Jung et al., 1994).

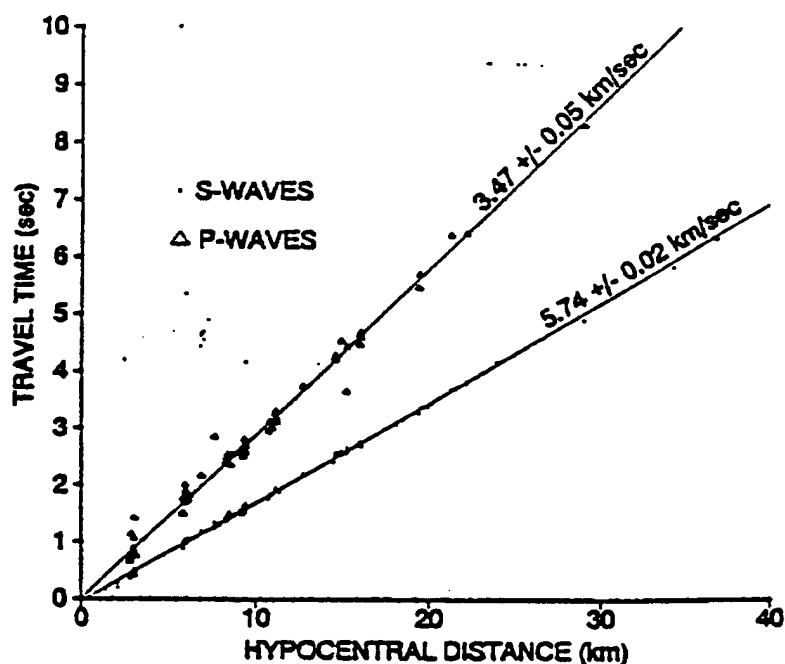


**Figure 2.** Travel time curve for seismic events in the Coeur d'Alene district based on independently known hypocentral locations.

Stopeing of the lead-zinc-silver ore in the district takes place on steeply dipping veins at an average depth of 1650 meters below surface. The country rock consists primarily of stiff, vitreous quartzite (Young's modulus = 55 GPa, uniaxial compressive strength = 300 MPa). There are also smaller pockets of sericitic quartzite and thin bands of argillite (both of which are considerably softer and weaker than vitreous quartzite). Scott et al. (1993) discussed the influence that these geological features may have on rockbursting. Based on overcoring measurements, observations of fracturing around raisebore holes, and natural earthquake data the maximum principal stress,  $S_1$ , is believed to lie approximately horizontal toward N40W (Whyatt et al., 1993; Sprenke et al., 1991). The magnitude of  $S_1$  is believed to be on the order of 1.5 to 3.0 times greater than the vertical stress. The magnitudes and orientations of the other two principal stresses,  $S_2$  and  $S_3$ , are less certain.

Three distinct types of seismic monitoring systems are used to monitor rockburst activity in the mining district (Williams et al, 1995). Electrolab MP250 microseismic systems were installed in the early 1970s to monitor rock popping around stopes. The U.S. Bureau of Mines installed in-mine 16-channel macroseismic monitoring systems in several mines since 1989. This mine-wide, digital, full-waveform system provides backup source locations as well as constraints on failure mechanisms and peak-particle

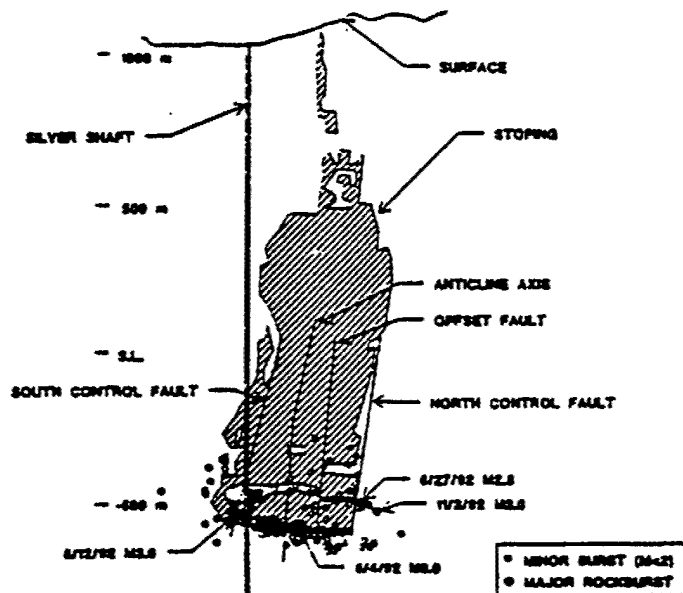


**Figure 3. Longitudinal section view of the Lucky Friday Mine showing rockburst hypocenters.**

ground velocities. The University of Idaho implemented a network of 16 surface seismographs covering the entire Coeur D'Alene mining district, from 1992-1994. All the surface seismometers were uncalibrated vertical component velocity gauges ranging in natural frequencies from 1 Hz to 4.5 Hz.



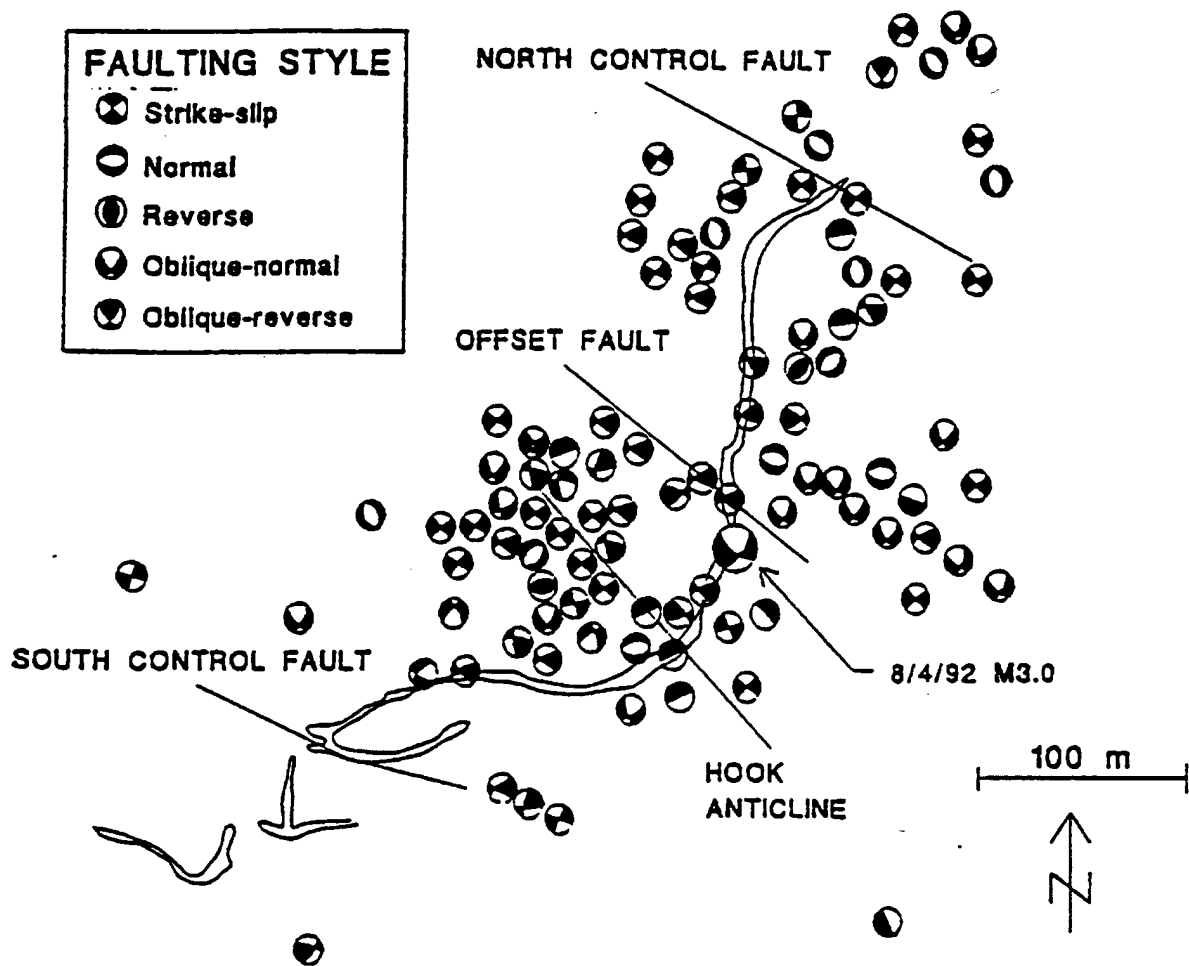
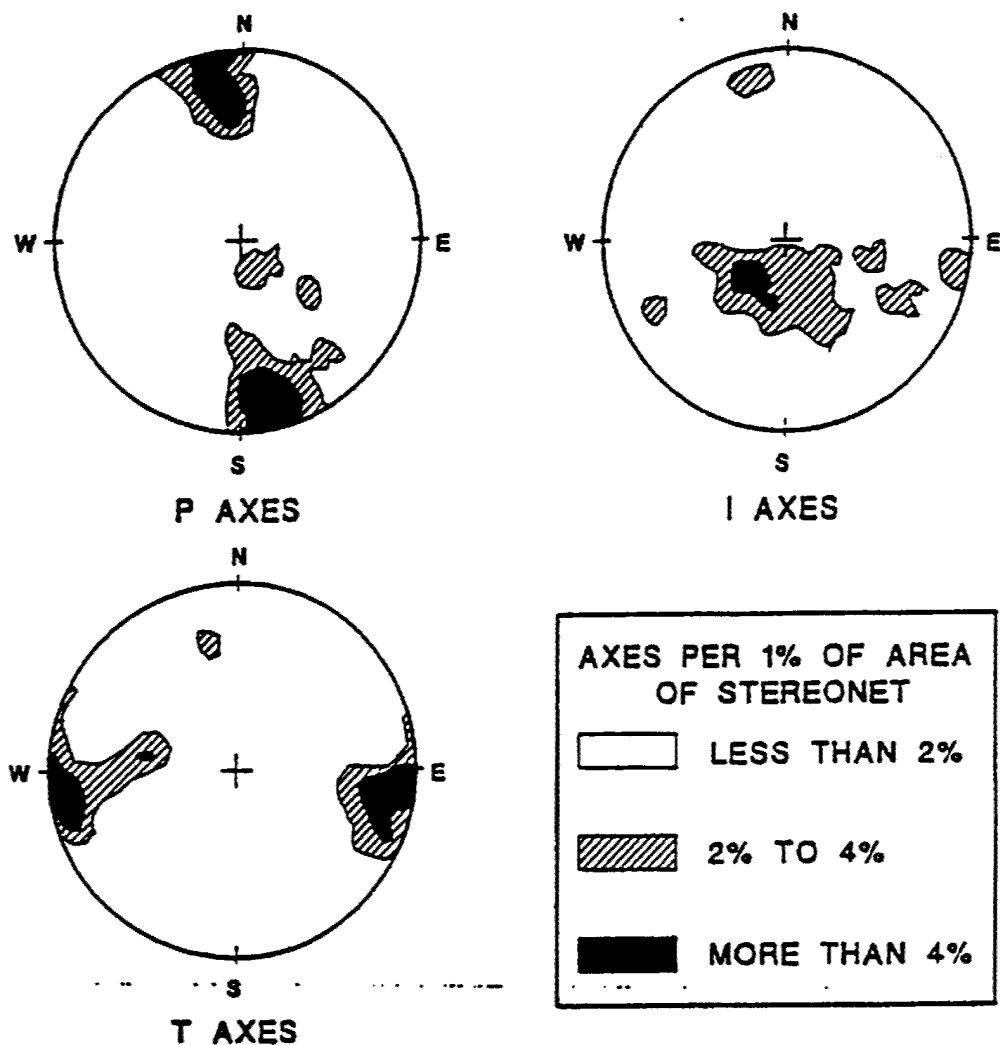


Figure 4. Fault plane solutions for events below the 5400 sub-level of the Lucky Friday Mine.

This network, in conjunction with a surface seismograph in the mineyard, provided complete focal-sphere coverage of seismic events at the Lucky Friday Mine, and allowed the computation of well-constrained fault plane solutions for most events above magnitude 0.5.

During the two-year deployment of the district-wide seismograph network, the mine seismograph recorded 1750 seismic events with hypocenter locations near the mine. The magnitudes of these events ranged from -1 to 3. The events were assigned locations from the in-mine rockburst monitoring systems. For most events, the source location is accurate to within 30 meters or less. Using data from our district-wide seismograph network, fault plane solutions were attempted for each of the 1750 seismic events recorded on the surface seismograph at the Lucky Friday Mine during a one-year period. Many of the events proved to be too small or too noisy to provide impulsive first motions on the far-field stations and some events resulted in ambiguous or poorly-constrained solutions. About half of the events had implosional source components (Stickney and Sprenke, 1993), producing dilatational first motions in all quadrants, making double-couple fault plane solutions impossible. In total, well-constrained fault plane solutions for 250 of the 1750 events. The definition of "well-constrained" was that there were no discrepant stations and that the possible solution planes fell in clusters within  $\pm 12$  degrees from their mean positions. Fault plane solutions were calculated by the program FPFIT (Lee and Valdes, 1985).



**Figure 5. Concentration contours for the P, I, and T axes plotted on equal area stereonets.**

In Figure 3, the locations of the shear-type seismic events are projected on a longitudinal section view of the bottom portion of the vein. Fault plane solutions corresponding to these events are shown in plan view (Fig. 4). The majority of the events occurred near the three bottom longwall stopes. Two types of fault plane solutions were found predominant: (1) randomly oriented normal or thrust faulting, and (2) strike-slip movement along vertical planes striking N45W or N45E. The magnitude 3 event located near the Offset fault shows right-lateral movement on a plane parallel to the fault. Also, several event clusters adjacent to the Offset fault all show the same strike-slip movement, located along a straight line parallel to the fault.

Because virtually all of the 250 shear events analyzed occurred in the vicinity of active stopes, the effect of near-field stress concentrations due to mine geometry was critical to the interpretation of each individual event. However, a general analysis of the fault plane solutions in conjunction with previous in situ measurements of stress orientations provided some interesting observations about the overall stress

regime in the mine. The respective groupings of the P, I, and T axes for all 250 well-constrained solutions were calculated using MicroNet (Guth, 1987), and are presented in lower hemisphere, equal area stereonets (Figure 5). These concentration plots indicate that the preferred seismic P-axis plunges near-horizontally with a bearing about N5W, and that the preferred seismic T-axis is near horizontal, bearing east-west. In terms of fault planes, this indicates the preferred failure plane is vertical and strikes either N50W or N40E. In terms of the geology of the mine, the most reasonable interpretation is that when large bursts occur, it is the three major, northwest trending, strike-slip faults and associated parallel fractures that tend to be re-activated in the vicinity of active stopes. It is generally easier to re-activate existing rupture planes than it is to create new fractures. The old fractures tend to have less cohesion and lower angles of friction than the surrounding intact rockmass. If the slip is in fact on pre-existing northwesterly trending fractures, the fault plane solutions show that the movement is nearly always right-lateral strike-slip with a smaller oblique components of normal or reverse faulting. Furthermore, because the S1 direction can lie anywhere from the 45° position of the seismic P axis to as close as 5° to the fault plane, the preferred P and T axes orientations are from 0° to 40° clockwise from the actual S1. Previous in situ measurements of S1 in and around the mine indicate a N40W orientation of S1, 35° from the seismic P axis and 10° from the failure plane, in the range one might expect for failure on pre-existing faults.

Composite analysis of the fault plane solution data and previous in situ stress measurements suggests that the overall stress regime in the mine is as follows: horizontal S1 oriented N40W, seismic P axis horizontal N5W, S2 vertical, S3 oriented horizontal N50E, and seismic T axis horizontal N50E. The overall preferred mode of failure for the shear events at the Lucky Friday Mine is right-lateral strike-slip movement along steeply dipping N50W striking planes. However, significant normal faulting along moderately dipping, northerly striking planes and thrust faulting along randomly striking, shallow dipping planes also occurs. Except for a few normal fault events on the 5100 level near the North Control fault, most of the fault plane solutions do not correlate well with the bedding plane orientations. Although the direction of maximum compression sometimes drifts to the vertical position resulting in gravity failures, the east-to-northeast extension direction is particularly persistent, being a feature of most of the fault plane solutions.

In a recent study (Whyatt et al., 1996), all available seismic data from the Lucky Friday Mine for the period 1989-1994 was analyzed to provide a foundation for assessing the seismic characteristics of large events in deep mines. Information was collected and analyzed for 39 seismic events with local magnitudes above 2.5. One of these events occurred, on average, every 8 weeks during the study period. The characteristic first motion patterns, damage patterns, and relationships to mining and geologic structure were defined for each event. However, other than the first motion fault plane solutions, no focal mechanism studies or moment tensor solutions have been obtained to date in the Coeur d'Alene district. Furthermore, no high quality broadband instruments have ever been deployed in or near the district.

#### 1.4 Objectives.

The objectives of this phase of the contract were

1. To deploy a local network of seismic sensors in a high rockburst region near existing mines in Northern Idaho.
2. To collect seismic data from this sensor network, from in-mine monitoring stations, and from regional and national networks at distances from tens to hundreds of kilometers.

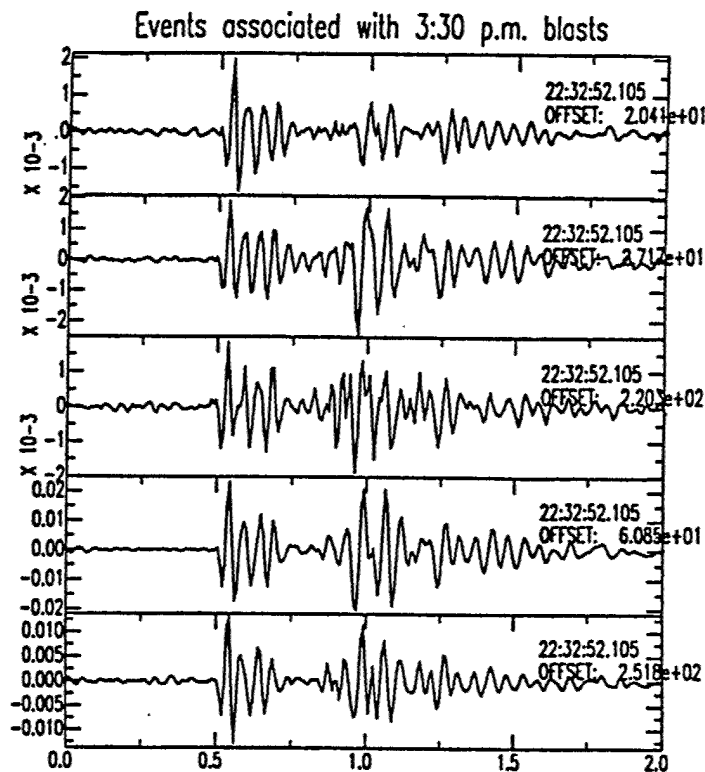


**Figure 6. Vertical Waveforms from Rockbursts Associated with Blasting at the Lucky Friday Mine.**

Locations and focal mechanisms determined from in-mine and regional seismic arrays indicate a significant implosional component (in addition to the usual shear component of natural earthquakes) for rockbursts and mine tremors in the Coeur d'Alene mining district (Figure 1) of northern Idaho (Sprenke et al., 1991; Stickney and Sprenke, 1993; Jung et al., 1995). A small, non-double-couple component seismic event at shallow depth (less than a few kilometers) may be difficult to discriminate from an explosion at regional distances. The initial P-wave polarity may not be determinable, the location and waveform characteristics will indicate a source in the shallow crust, and the relative amplitudes of compressional and shear waves may be similar to that of an explosion. There have been an average of approximately two seismic events per year since 1990 (Table 1) from the Lucky Friday mine that have magnitudes larger than 3 and these events could be detected by CTBT monitoring systems.

**Table 1. Event catalog from the Composite National Seismic System**

Date	Time	Lat	Long	Depth	Mag
3/7/1990	21:54.4	47.453	-115.974	1.7	3
6/13/1991	03:36.7	47.852	-115.713	7.5	3
9/19/1991	20:27.8	47.458	-115.803	1	3
12/11/1991	37:03.4	47.48	-115.801	1	3
8/4/1992	26:28.9	47.468	-115.785	2	3.2
8/12/1992	30:23.4	47.469	-115.78	2.3	3.2
11/4/1992	21:42.7	47.467	-115.775	2.2	3
3/18/1993	00:53.1	47.472	-116.015	9.6	3.1
7/1/1993	48:00.5	47.477	-116.108	1	3.2
10/18/1993	49:10.1	47.471	-115.783	1	3.3
3/8/1994	07:11.5	47.186	-115.932	5	3.4
8/17/1994	56:49.0	47.472	-115.778	1.6	4.1
4/25/1996	56:29.1	47.443	-115.816	1	3
5/30/1996	00:37.8	47.44	-115.82	1	3.6
11/2/1996	28:26.3	47.798	-115.642	5	3.6
3/14/1997	18:32.0	47.47	-115.78	2	3.6

This project obtained the first high-quality seismic data to determine the source characteristics and moment tensors of seismic events in this region. This is the first time a broad-band, high dynamic-range, three-component instrument has been operated in this mining district.

**Table 2. Event Catalog from the In-Mine Monitoring System**

DATE	TIME	X	Y	Z	AMPL (mm)	STOPE	ML
7/30/1998	1:20:28	232	-164	-2750	7	575-05	
7/30/1998	16:24:12	287	-1000	-2564	4	550-01	
7/30/1998	23:40:13	-397	-100	-2750	3	575-05	
7/31/1998	1:33:09	-356	-307	-2750	4	575-05	
7/31/1998	5:25:36	-396	-1000	2750	10	550-01	
7/31/1998	23:35:54	-988	-460	-2750	4	550-01	
8/1/1998	5:53:22	-258	-71	-2715	3	575-05	
8/2/1998	1:52:25	-220	-90	-1463	6	49-87	
8/3/1998	9:12:44	-218	-736	-2760	2	550-01	
8/4/1998	20:44:42	-92	-763	-2750	3	550-01	
8/4/1998	21:29:38	1793	108	-1380	5	46-110	
8/4/1998	22:18:09	-663	-320	-2750	2	550-01	
8/5/1998	0:39:29	-177	723	-2750	14	593-ramp	
8/5/1998	23:31:47	-169	587	-2750	4	593-ramp	
8/6/1998	7:25:31	-54	-512	-2585	74	575-05	1.2
8/6/1998	18:19:23	156	-1000	-2750	5	550-01	
8/8/1998	1:54:56	-1048	2352	-1726	76	paymaster	1.4
8/10/1998	23:37:42	-255	496	-2750	3	593-ramp	
8/10/1998	23:38:54	220	-166	-2750	2	584-06	

Table 2. Event catalog from the in-mine monitoring system (cont.)

DATE	TIME	X	Y	Z	SIZE MM	STOPE	ML
8/11/1998	11:27:33	-6	-205	-2750	4	575-05	
8/12/1998	13:32:46	-33	197	-2750	3	575-05	
8/13/1998	3:59:22	-729	-415	-2750	16	550-01	
8/13/1998	8:54:49	1146	70	-1989	5	557-08	
8/13/1998	14:35:49	-32	-312	-2750	2	575-05	
8/14/1998	2:54:31	-1445	3150	-1638	16	gold hunter	
8/16/1998	1:05:42	-255	-980	-2423	2	550-01	
8/18/1998	11:25:28	183	-162	-2433	80	575-05	1.5
8/18/1998	17:18:34	-281	-70	-2750	2	575-05	
8/18/1998	23:39:14	6	-47	-2323	2	575-05	
8/19/1998	22:51:55	-153	-438	-2750	2	575-05	
8/20/1998	13:42:43	-161	-107	-2750	16	575-05	
8/20/1998	13:42:57	-248	-146	-2750	10	575-05	
8/20/1998	14:09:26	-106	87	-2750	10	575-05	
8/20/1998	20:18	93	-261	-2378	3	575-05	
8/21/1998	31:35:00	124	-286	-2419	70	575-05	1.1
8/21/1998	31:38:00	-137	-228	-2749	12	575-05	
8/21/1998	34:23:00	152	-66	-2750	3	584-06	
8/21/1998	36:47:00	139	-890	-2750	2	550-01	
8/22/1998	38:26:00	-335	-306	-2750	14	575-05	
8/22/1998	33:59:00	-323	-200	-2750	6	575-05	
8/24/1998	11:12:13	1985	1605	-1322	16	3250 ncf	
8/24/1998	16:04:47	511	299	-2584	3	584-07	
8/25/1998	13:35:19	-342	4	-2750	4	575-05	
8/25/1998	23:36:01	-200	-168	-2752	9	575-05	
8/26/1998	0:18:48	165	-195	-2750	8	575-05	
8/26/1998	13:55:57	-235	-140	-2731	70	575-05	0.8
8/26/1998	14:12:32	-193	-247	-2716	20	575-05	
8/27/1998	0:08:09	-154	-168	-2750	10	575-05	
8/27/1998	0:57:41	-320	-311	-2750	14	575-05	
8/27/1998	14:47:24	-130	-220	-2738	10	575-05	
8/28/1998	0:24:03	-42	-195	-2750	5	575-05	
8/28/1998	7:54:22	-160	-36	-2081	5	557-04	
8/28/1998	13:35:40	203	-9	-2750	4	575-05	
8/28/1998	13:49:50	19	-307	-2547	12	575-05	
8/28/1998	13:53:29	83	46	-2348	4	575-05	
8/28/1998	19:13:15	-82	-347	-2750	4	575-05	
8/28/1998	23:09:27	53	-73	-2075	80	575-05	3.1
8/28/1998	23:24:16	357	81	-2750	10	584-06	
8/28/1998	23:27:41	98	-65	-2750	3	575-05	
8/29/1998	7:26:56	50	-237	-2750	8	575-05	
8/29/1998	9:07:36	-216	-432	-2750	2	575-05	
8/29/1998	13:56:06	1514	-37	-2750	6	584-06	
8/30/1998	18:57:40	-600	29	-2750	10	5900	
8/31/1998	11:53:25	14	55	-2309	6	575-05	

### 1.5 Seismic Data from Sensor Network and from In-mine Stations.

We operated five strong-motion accelerometers and one broadband seismometer within about 5 km of the Lucky Friday mine during the summer of 1998. The strong motion accelerometers recorded 2-10 of the larger rockbursts per week of operation; the broadband instrument recorded about 20-40 per week. We have collected about 24 weeks of data from the broadband seismometer and about 14 weeks of data from the strong motion accelerometers (Table 2). Many of the events occurred at or near the time explosions were used to create new openings in the mine (Table 3), but most waveforms indicate implosional first motions. The explosions were usually too small to be observed, and the implosional events often occurred several minutes after the blasting time. Figure 6 shows examples of the waveforms obtained on the broadband system for events occurring near the blast times. Figure 7 shows the displacement spectra obtained from 26 events that all had similar waveforms and dilational first motions at this site. The use of broad-band, high dynamic range accelerometers produced very high quality, on-scale recordings of rockbursts at distances as short as 2 km and magnitudes up to 2.

The Lucky Friday survey system is (X,Y,Z) where X = Easting (ft), Y = Northing (ft), and Z = Elevation (ft). Conversion from mine coordinates to geodetic survey coordinates is described in Table 4. Some mine maps will show coordinates with 20000 added to X and Y, so the origin used by the MP250 is technically at (20000,20000,0) on these maps. The X and Y used in the conversions below should NOT have the 20000 added. Note that most bursts will be at negative elevations. The elevation of the surface seismograph at the mine is 3360 feet above sea level.

**Table 3: Blast times for mines in the Coeur d'Alene District**

Gold Hunter Mine	115 am PDT	0815 UTC
Lucky Friday Mine	130 am PDT	0830 UTC
Gold Hunter Mine	1100 am PDT	1800 UTC
Gold Hunter Mine	315 pm PDT	2215 UTC
Lucky Friday Mine	330 pm PDT	2230 UTC
Gold Hunter Mine	900 pm PDT	0400 UTC

**Table 4: Mine coordinates**

LATITUDE	$0.0001638 \cdot Y + 47 \text{ degrees } 28.18 \text{ minutes}$
LONGITUDE	$115 \text{ degrees } 46.90 \text{ minutes} - 0.0002427 \cdot X + 0.000004 \cdot Y$
ELEVATION (meters)	$Z \cdot 0.3048$

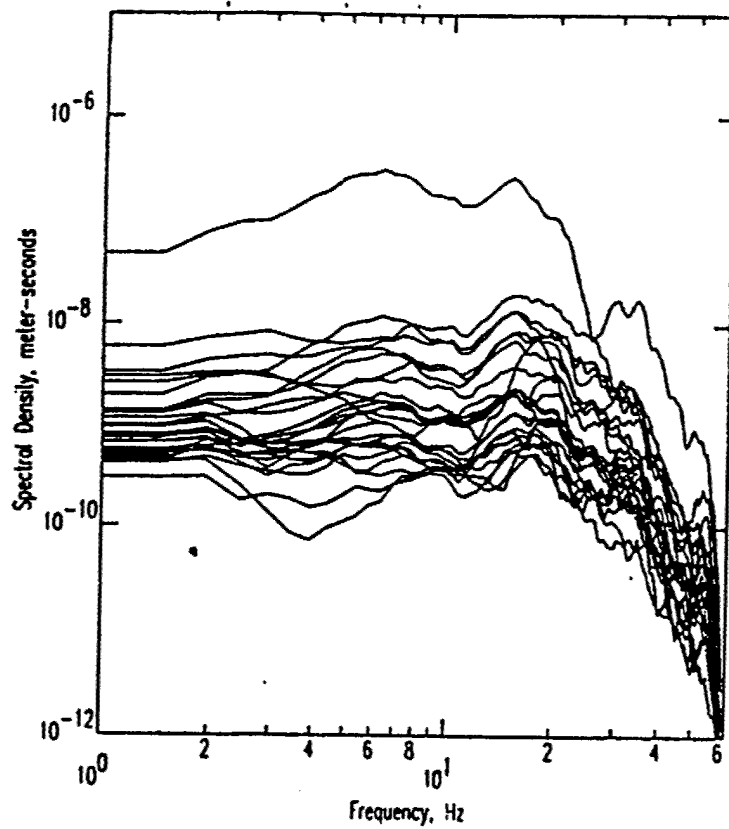


Figure 7. Displacement amplitude spectra of 26 signals with dilatational first motions.

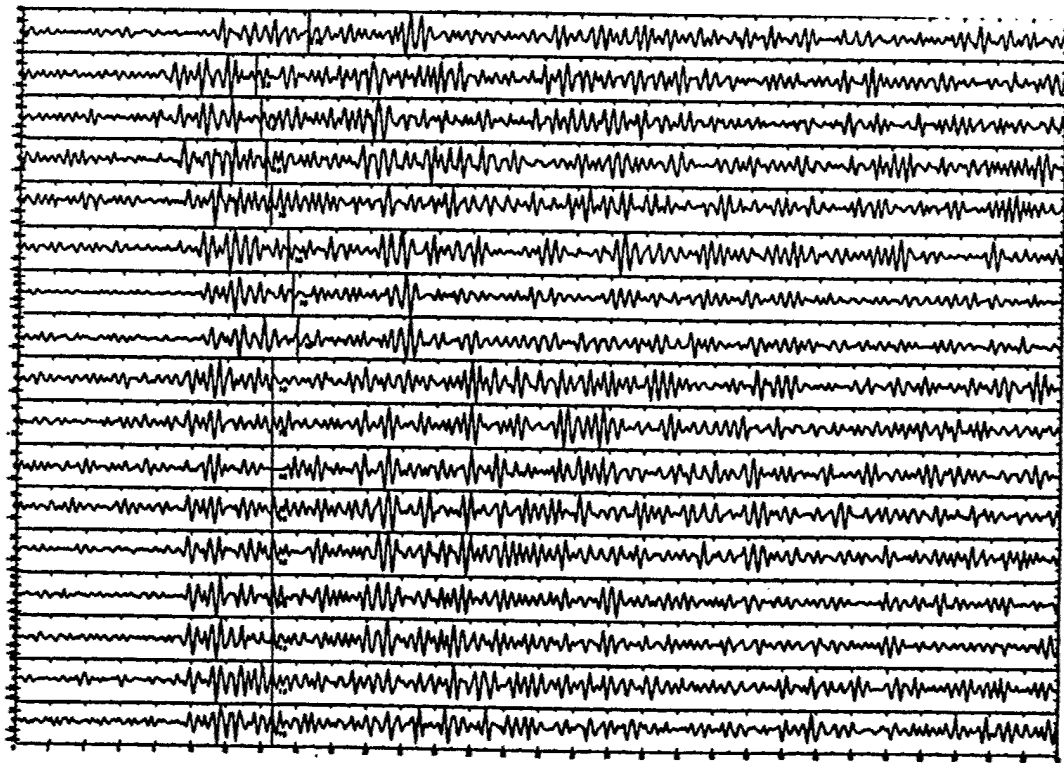


Figure 8. Waveforms recorded at the Yellowknife Array, 1500 km north of the Lucky Friday Mine.



## 1.6 Data from Sources at Regional Distances.

We have also obtained some regional waveforms from North American stations that are elements or possibly auxiliary elements of the CTBT monitoring system. Figure 8 shows the waveforms recorded at the Yellowknife array from an event at the Lucky Friday mine in 1996. Data from other North American broadband stations, and regional arrays operated in eastern Washington, northern Idaho, and western Montana, were assembled to evaluate wave propagation characteristics and the development of regional phases from seismic events in the study region. A catalog of all known recorded rockbursts in the northern Idaho region is given in Table 5 below.

The Montana Bureau of Mines and Geology (MBMG) records a network of seismograph stations operated in southwest Montana and collects trace data from two smaller networks operated in west-central and northwest Montana. Together these three groups of seismograph stations comprise the Montana regional seismograph network. Local and regional earthquakes were visually identified on seismograms and P and S arrival time were picked if three or more stations record first-arriving P-waves. Mining and construction blasts were discriminated on the basis of seismogram appearance, time of day, and source proximity to known mining or construction areas. Hypocenter locations were determined for all seismic events that could not be confidently identified as blasts and are included in the MBMG earthquake catalog. Phase data were collected from seismograph stations operated in surrounding areas by other institutions. Surrounding seismograph stations include those operated by the US National Network Station at Newport, WA, the University of Washington, the University of Idaho, the Army Corps of Engineers, Boise State University, the Idaho National Engineering and Environmental Laboratories, surface mine seismographs at three mines in the Coeur d'Alene mining district operated by various mining companies and the U.S. Bureau of Mines, and various stations in southern British Columbia and southern Alberta operated by the Canadian Geological Survey. Of course not all of these stations operated during the same time periods. Seismograph coverage in the Northern Rocky Mountain region has generally improved over the past 18 years however, the best seismic coverage of the Coeur d'Alene mining district existed while the North Idaho seismic network was operational in the early 1990s.

P and S arrival times were initially read from paper seismograms recorded at a rate of 60 mm/second for an overall timing accuracy of 0.1 seconds. After August of 1989, Montana network stations were digitized at 100 samples/second and recorded on a PC-based data acquisition in Butte. XRTP (Tottingham, 1994), the data acquisition software operated in a triggered mode. Events that triggered were picked using PC-SUDS software (Banfill, 1996) for an overall timing accuracy of 0.02 seconds for impulsive arrivals. When the Flathead network became operational in 1996, XRTP was used to record seismic events. XRTP was also installed in Missoula at about this time to record west-central Montana seismic data. In 1998, both recording sites were upgraded to ViSeis data acquisition software. Phase data from all available seismograph stations were used with the Montana crustal velocity model (Stickney, 1997) and the hypocenter location programs HYPO71 (Lee and Lahr, 1975) and HYPO71PC (Lee and Valdes, 1985) to determine hypocenter locations. Magnitudes were determined from coda length measurements using the method described by Stickney (1995). When visible signals were recorded on the Butte Wood-Anderson equivalent seismograph, local (Richter) magnitudes were also determined. Magnitudes determined from both methods for individual events generally agree within one quarter of a magnitude unit.

A search of the MBMG earthquake catalog of an area 10 km in radius around the Lucky Friday Mine (47.471°N, 115.783°W) yielded 86 seismic events (Table 5). All are believed to be seismic events directly associated with the Lucky Friday Mine. Mine operators confirmed that many of these events were rockbursts. Of these 86 events, two resulted in casualties to underground miners, and 19 were reported as being felt by people at the surface, although many more were undoubtedly felt but not so reported. The cataloged Lucky Friday Mine seismic events since 1982 range in magnitude from 1.5 to 4.1 although the detection threshold for the Montana regional seismograph network alone is about magnitude 2.3. A total

of 18 events have magnitudes of 3.0 or greater, 6 are 3.5 or greater and 1 exceeds magnitude 4.0. From 1996 through 1999, on average, 8.8 Lucky Friday events are detected and located annually with regional network data.

**Table 5. Regional Rockburst Catalog (1982-1999)**

Date	hr-min	sec	Latitude	Longitude	Depth (km)	Magnitude
83 10 15	1115	10.3	47.485	115.79	0.2	2.5
84 1 19	725	47.1	47.401	115.839	0.4	3.1
84 1 25	1936	11	47.488	115.734	11	2.9
85 1 20	118	24.6	47.526	115.767	1	2.8
85 2 8	1422	19	47.469	115.81	4.4	3.2
85 4 13	510	31	47.439	115.817	0.1	1.7
85 9 12	2134	40.5	47.484	115.775	9.5	1.5
85 10 31	1131	50.9	47.514	115.751	4.7	3
85 12 4	2340	51.9	47.494	115.776	6.3	3.2
85 12 10	1858	43.5	47.413	115.867	0.2	2.7
86 1 9	634	53.8	47.477	115.771	6.4	2.9
86 1 28	1324	0.3	47.486	115.722	7.5	2.8
86 1 30	2239	26.4	47.506	115.722	5.7	2.8
86 3 5	1939	42.7	47.483	115.749	0.6	2.1
86 3 12	1632	56.7	47.46	115.802	0.1	2.6
86 3 25	2207	38.8	47.472	115.746	1.3	2.3
86 5 13	506	6	47.453	115.9	1.8	2.5
87 11 19	637	29.6	47.456	115.838	2.6	2.6
87 11 28	321	35.6	47.499	115.772	14.8	2.4
88 2 3	1506	52.5	47.427	115.747	1.2	2.4
88 10 7	540	27.4	47.428	115.887	10.6	2.5
88 10 18	2115	1.7	47.463	115.826	8.3	3.7
89 4 4	1042	59.3	47.462	115.846	7.1	3.1
89 4 13	1323	32.8	47.464	115.853	9	2.5
89 7 6	707	56	47.462	115.839	8.9	3.7
89 10 16	1101	7	47.472	115.863	9.3	2.6
89 11 3	631	1.1	47.459	115.814	4.2	2.8
90 3 31	703	5.7	47.425	115.84	3.5	2.4
90 4 11	422	42.9	47.468	115.77	0.9	2.6
90 6 12	2104	56.2	47.455	115.804	2.9	2.5
90 8 3	1639	13.8	47.471	115.783	1.5	2.8
91 2 23	652	13.1	47.434	115.853	13.9	3
91 3 1	409	25.6	47.42	115.694	14.9	2.8
91 5 9	1918	7	47.472	115.842	8.7	2.8
91 5 17	734	16.4	47.45	115.806	3	2.7
91 8 17	832	51.3	47.452	115.892	9.7	2.9
91 9 19	1620	28.8	47.455	115.826	3.4	3.5
91 12 11	2137	0	47.5	115.8	2	3.2
92 7 30	738	20.8	47.468	115.785	2.2	2.8
92 8 4	926	28.9	47.468	115.785	2	3.2
92 8 12	830	23.4	47.469	115.78	2.3	3.2
92 11 4	521	42.7	47.467	115.775	2.2	3
93 10 18	649	10.1	47.471	115.783	1	3.3
94 8 17	656	50.3	47.472	115.778	1.6	4.2
94 9 28	342	7	47.471	115.783	2	2.8
94 12 4	455	59.8	47.471	115.77	2	2.8

**Table 5. Regional Rockburst Catalog (1982-1999) (Continued)**

Date	hr-min	sec	Latitude	Longitude	Depth (km)	Magnitude
95 1 13	836	5.8	47.471	115.783	2	2.8
95 4 26	1414	5.7	47.471	115.783	2	2.7
95 5 27	1117	21.5	47.471	115.783	2	2.7
95 6 23	438	17.3	47.44	115.855	2	3.3
95 9 19	2040	36.9	47.471	115.783	2	2.7
96 2 9	201	29.3	47.457	115.84	0.2	3.7
96 4 25	2056	29.8	47.445	115.807	0.3	3
96 5 30	1000	38.8	47.471	115.783	2	3.8
96 9 26	2137	48.2	47.471	115.783	2	2.1
96 9 26	2259	28.5	47.471	115.783	2	2.6
96 11 2	240	26.6	47.468	115.845	2	2.7
96 12 20	838	37.2	47.471	115.783	2	2.3
97 2 14	837	55	47.471	115.783	2	2.5
97 3 14	1718	32.8	47.471	115.783	2	3.8
97 3 27	2109	22.1	47.46	115.864	2	2.1
97 4 26	558	28.5	47.542	115.726	4.5	2
97 5 25	1534	8.5	47.471	115.783	2	2.6
97 6 28	302	38.8	47.471	115.783	2	3.5
97 8 22	2128	15.9	47.471	115.783	2	2.4
97 9 5	2146	16.6	47.471	115.783	2	2.2
97 9 24	2250	21	47.471	115.783	2	2.1
97 11 8	1333	14.9	47.415	115.818	1.5	1.9
97 11 12	2314	14.9	47.48	115.763	2	2.1
98 1 30	840	40.4	47.471	115.783	2	2.6
98 2 19	2336	43.3	47.471	115.783	2	2.9
98 3 6	1811	43.4	47.471	115.783	2	2.8
98 3 18	937	32.2	47.471	115.783	2	2
98 4 5	1200	18.3	47.471	115.783	2	2.5
98 5 4	2237	35.9	47.471	115.783	2	2.1
98 5 14	834	18.4	47.471	115.783	2	2.1
98 8 29	609	27.2	47.454	115.833	2	3
98 12 9	2207	16.7	47.471	115.783	2	2
98 12 18	2316	52.2	47.471	115.783	2	2.1
99 1 25	2214	16.4	47.471	115.783	2	2.1
99 6 12	1843	13.1	47.471	115.783	2	3.2
99 7 8	2042	51.6	47.471	115.783	2	2.9
99 10 23	2216	56.2	47.475	115.805	2	2.5
99 10 28	707	24	47.469	115.806	2	3
99 11 2	847	46.8	47.489	115.777	2	2.4
99 12 17	1025	26.3	47.436	115.827	2	2.8

## SECTION 2

### SEISMIC SOURCE PARAMETERS OF ROCK BURSTS COEUR D'ALENE MINING DISTRICT, IDAHO

#### 2.1 Introduction.

Characterization of mining-related seismic events is critical to the implementation of the Comprehensive Nuclear Test-Ban Treaty monitoring system. Mine seismicity from uncontrolled sources are particularly troublesome, with magnitudes up to 4 or 5, producing signal strengths comparable to 1-10 kiloton contained nuclear explosions. In this study, ground motions from four surface stations and one underground station (Figure 9) were inverted to determine the complete moment tensor of a relatively large rock burst in the Coeur d'Alene Mining District in northern Idaho. Many rock bursts, induced by the mining process, show shear implosional source mechanisms, a feature that should be useful to discriminate mining-related events from underground explosions.

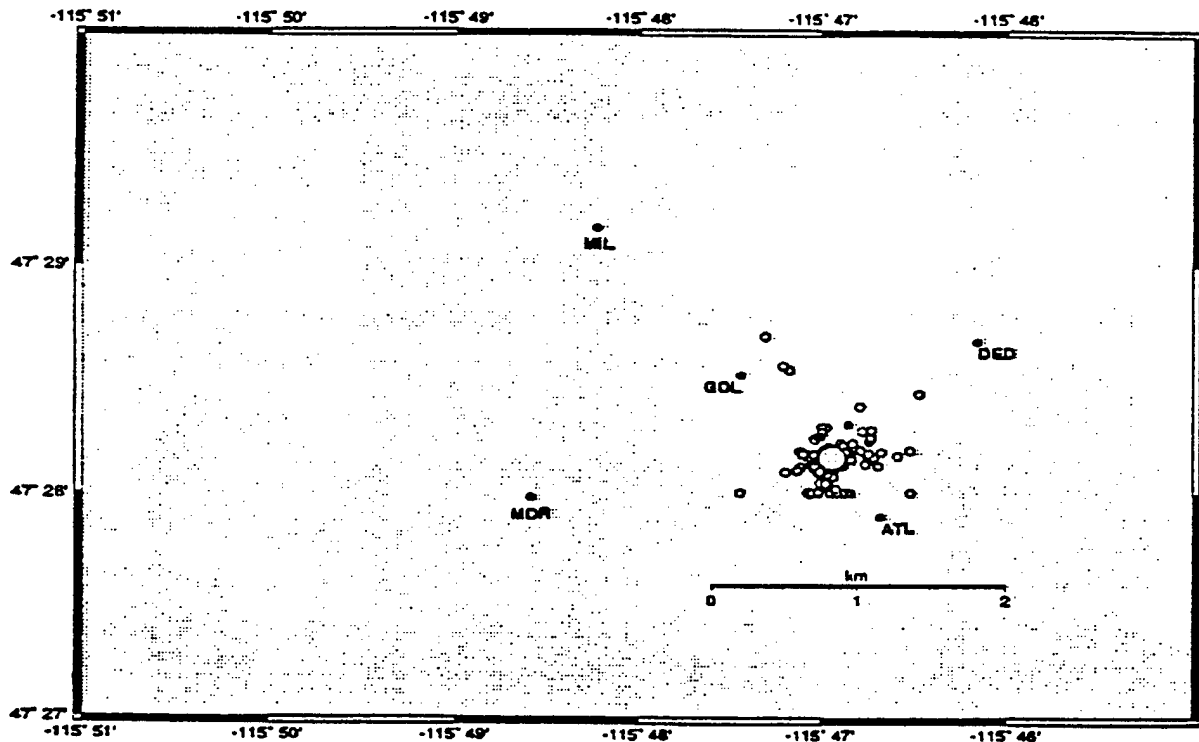


Figure 9. Locations of stations and of larger events recorded.

#### 2.2 Objective.

The objective of this portion of the study was to apply modern methods and techniques to determine the seismic source parameters of rockbursts. Mining activities world-wide produce seismic events, some of which may be visible to monitoring for the Comprehensive Test Ban Treaty (CTBT). Mine seismicity from uncontrolled sources are particularly troublesome, with magnitudes as high as 4 to 5, producing signals equivalent to 1-10 kiloton contained nuclear explosions. Rock bursts in deep underground mines

are in this latter category. These events, however, may have characteristics unlike either explosions or earthquakes that might be used to “fingerprint” specific mines for discrimination purposes. In this light, we are investigating seismic signals from one of the most rock burst-prone hard rock mining areas in the world: the Coeur d’Alene Mining District of Northern Idaho.

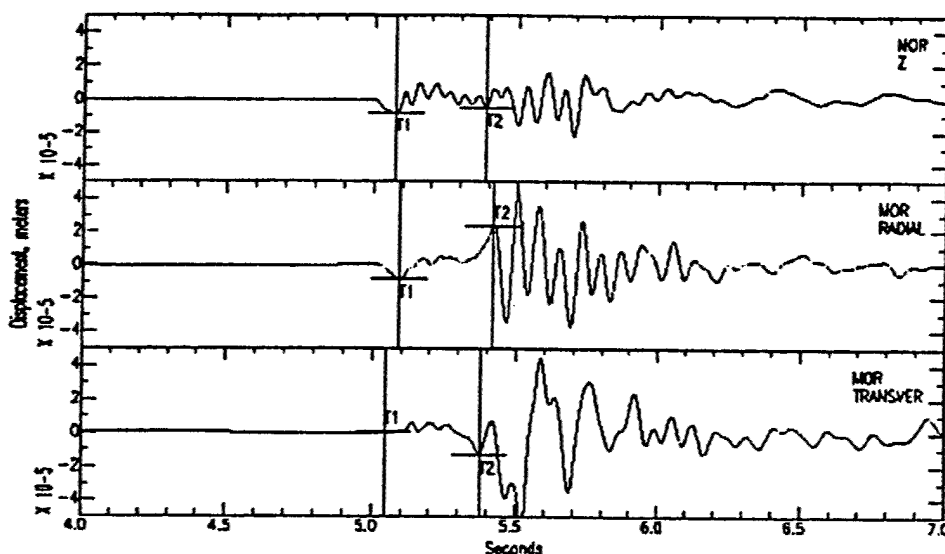


Figure 10. Displacements recorded at MOR for the largest rockburst recorded.

In a review of mining-induced seismicity, Gibowicz and Kijko (1994) note that such events generally fall into two types—those directly associated with mining operations and those associated with movement on major geological discontinuities. Rock bursts in the Coeur d’Alene District are not so easily categorized. While the events clearly are associated with mining rate (Sprenke and others, 1991) and stope geometry (Jung et al., 1995), they have long been known to be the result of failure on faults and bedding planes (Scott, 1990) associated with the Osburn Fault, part of the Lewis and Clark Line megashear that strikes north-northwest through the district. An underhand-longwall system of mining, implemented in the late 1980s at the Lucky Friday Mine, has greatly reduced rock burst problems at that mine, illustrating the influence of mining geometry on rock bursts. A district-wide network operated in the early 1990s (Jung et al., 1995) showed that those shear events that could be fit by a double couple solution were consistent with a regional tectonic stress with a northwesterly oriented seismic P-axis and and northeasterly seismic T-axis, an orientation particularly deleterious for slip on the north-northwesterly oriented vertical faults and steeply-dipping bedding parallel to the Osburn Fault. Apparently, mining operations in the Coeur d’Alene district are releasing pent-up strain, strongly affected by local geology and tectonics. Not unlike deep mines world-wide, the seismicity in this district are affected by depth of mining, production rate, mining geometry, geologic structure, and geologic discontinuities.

Although blasting often triggers rock bursts instantaneously, many rock bursts, particularly large damaging events in deep underground mines, occur spontaneously and unexpectedly—this despite the fact that they are caused by stress changes associated with the mining process. This interaction of mine geometry and geological structure suggests that rock bursts in deep underground mines may often be of a shear-implosional nature, involving both co-seismic opening closure and shear failure in the surrounding strata (e.g. McGarr, 1992). Seismograph networks (Stickney and Sprenke, 1992; Jung et al., 1995)

demonstrated that well-constrained all-dilatational P-wave first motions for about half of the events in the Lucky Friday Mine indicated a significant implosional component.

For this project, we have investigated the seismic signals from a damaging rock burst in the Lucky Friday Mine. The local magnitude of the event was 3.1 as measured at Butte, Montana. It was recorded on the Montana and Washington region networks. Predominantly dilatational first motions for this event from our five local stations and several regional stations suggested that this event had an implosional component. The following source parameters were estimated from the events far field displacement spectrum as measured on the broadband instrument at station MOR (Figures 9 and 10).

### 2.3 Seismic Moment.

The strength of a seismic event is commonly defined in terms of a double-couple point source model. More complex source characteristics will be considered later in this paper when the seismic moment tensor is computed for the events. The seismic moment  $M_0$  is the usual parameter used to express the size of a seismic event. Moment is defined by  $M_0 = \mu u A$  where  $\mu$  is the shear modulus,  $u$  is the average slip of the fault, and  $A$  is the area of the fault. For large events,  $M_0$  can be calculated directly from field estimates of fault displacement and fault area, but usually  $M_0$  has to be estimated using seismic records in the frequency domain using the following formula:

$$M_0 = 4 \pi c^3 R \Omega_0 F_C^{-1} R_C^{-1} S_C^{-1} \quad (2.1)$$

where

- $c$  = velocity of P waves ( $\alpha$ ) or S waves ( $\beta$ ) at the source,
- $R$  = hypocentral distance,  $\Omega_0$  is the low frequency limit,
- $F_C$  = the radiation factor,
- $R_C$  = the free surface effect,
- $S_C$  = the site correction. For the broadband station MOR (Figure 9) used in this study,
- $R$  = 2660 m,
- $\alpha$  = 5740 m/s,
- $\beta$  = 3470 m/s,
- $F_{C\alpha}$  = 0.52,
- $F_{C\beta}$  = 0.63,
- $RC\alpha$  = 1.05, and
- $RC\beta$  = 2.

The low frequency limit  $\Omega_0$  can be measured directly on the far field displacement spectrum or can be found by integrating the displacement pulse in the time domain. For our largest event,  $\Omega_0$  for P was found to be  $1.1 \times 10^{-7}$  m-s and for S was  $1.4 \times 10^{-6}$  m-s. The corresponding seismic moments were calculated as  $3.4 \times 10^{12}$  N-m and  $4.2 \times 10^{12}$  N-m respectively. For comparison, as described later, the moment tensor estimate of  $M_0$  is about  $5 \times 10^{13}$  N-m.

## 2.4 Moment Magnitude.

Moment magnitude  $M_w$  is commonly used as a measure of seismic event size. The definition of this magnitude scale is as follows:

$$M_w = 2/3 \log M_0 - 6.07 \quad (2.2)$$

where  $M_0$  is expressed in N-m (Kanamori and Hanks, 1979). For the largest rockburst in our study,  $M_w$  was calculated from our values of  $M_0$  as 2.4. For comparison, the magnitude was measured on the Richter scale as ML 2.9 (Butte).

## 2.5 P-Wave and S-Wave Energy.

The radiated elastic energy  $E_c$  by P or S-waves is another measure of the size of a seismic event. The radiated energy can be approximated as follows:

$$E_c = 4 \pi \rho c \langle F_c \rangle^2 R^2 F_c^{-2} R_c^{-2} J_c \quad (2.3)$$

where

$c = \alpha$  or  $\beta$ , and

$\langle F_c \rangle^2 =$  the mean square radiation coefficients, 4/15 for  $\alpha$  or 2/5 for  $\beta$ .

The other parameters are as defined above, and:

$$J_c = 0.25 \Omega_0^2 (2 \pi f_0)^3 \quad (2.4)$$

where  $f_0$  - the corner frequency of the displacement spectrum.

For the largest event in our data set, we found  $f_0 = 20$  Hz for the P wave and 14.8 Hz for the S wave. Using other parameters as given above, the P and S radiated energy were found to be 1500 N-m and 39,000 N-m, respectively. The ratio of  $E_s$  to  $E_p$  for the event was about 26, quite a high ratio considering the implosional nature of the source. Rockbursts are said to be commonly depleted in S waves with  $E_s$  to  $E_p$  ratios as low as 1.5 (Gibowicz et al., 1990).

## 2.6 Radiation Efficiency.

Rockbursts in mines are thought to have low seismic efficiency. Only a few per cent, at most, of the rupture energy seems to be released by seismic waves (McGarr, 1976; McGarr et al., 1979). Most of the energy is lost as heat. The radiation efficiency  $\epsilon_c$  is a measure comparing radiated seismic energy for P or S waves to dynamic stress drop ( $\sigma_{rms}$ ) at the source:

$$\epsilon_c = \mu E_c M_0 / \sigma_{rms} \quad (2.5)$$

where  $\mu$  = shear modulus.

The dynamic stress drop is calculated from  $a_{\text{RMS}}$ , the root mean square acceleration averaged over the duration of the S wave arrival as follows:

$$\sigma_{\text{RMS}} = 3.2 \rho R a_{\text{RMS}} (f_s / f_{\text{MAX}})^{1/2} \quad (2.6)$$

where

$f_s$  = S wave corner frequency on the displacement spectrum, and

$f_{\text{MAX}}$  = highest frequency of acceleration reliably recorded.

For the largest rockburst recorded in our study, we found  $a_{\text{RMS}} = 0.11 \text{ m/s}^2$ ,  $f_s = 14.8 \text{ Hz}$ ,  $f_{\text{MAX}} = 80 \text{ Hz}$  and  $\sigma_{\text{RMS}} = 1.08 \times 10^6 \text{ Pa}$ . The radiation efficiency for P and S waves was found to be  $1.33 \times 10^{-5}$  and  $2.82 \times 10^{-4}$ , respectively.

## 2.7 Source Dimensions.

Estimates of source dimension are commonly made assuming the Brune (1970) model, for which the area of a circular fault is inversely proportional to S wave corner frequency:

$$2\pi r_0 = 2.34 \beta / f_0 \quad (2.7)$$

where  $r_0$  is the radius of the fault. This relation assumes an instantaneous stress release.

For the largest rockburst in our data set, the source size worked out to be 87 m using the simple Brune model. It must be noted, however, as McGarr (1984, 1991) points out, that, although displacement may occur over the entire source dimension, the actual damage in mines would occur over a much smaller area where asperities along the fault exist.

## 2.8 Pulse Duration and Rupture Velocity.

An estimate of the upper limit of rupture velocity can be made from  $\tau$ , the pulse duration of ground velocity.

$$V = 12 r_0 / (16 \tau + 13 \xi) \quad (2.8)$$

where

$$\xi = r_0 \sin \theta / \beta.$$

The angle  $\theta$  is the take off angle measured from the normal to the fault plane. If  $\theta = 0^\circ$ , then the upper limit of rupture velocity can be estimated. For our largest rockburst, the takeoff angle  $\theta$  is close to  $0^\circ$ . The rupture velocity comes out at 1770 m/s or about  $0.51 \beta$ , somewhat slower than natural earthquakes which have rupture velocities from  $0.6 \beta$  to  $0.9 \beta$ .



## 2.9 Stress Drop.

The difference between the initial and final stress levels over a fault plane is called the static stress drop. However, seismic data can really only measure the dynamic stress drop, the difference between the initial stress level and the kinetic friction level on the fault.

The most common estimate of stress release during a seismic event is the Brune Stress Drop  $\Delta\sigma$  calculated from:

$$\Delta\sigma = 7/16 M_0 / r_0^3 \quad (2.9)$$

The Brune Stress Drop is an approximation of the static stress drop and it represents the uniform reduction in shear stress acting to produce seismic slip over a circular fault. For the largest rock burst in our data set,  $\Delta\sigma$  works out to be 2.7 Mpa.

## 2.10 Apparent Stress.

The apparent stress  $\sigma_A$  is another seismic measure of stress release (Wyss and Brune, 1968). It is calculated from radiated P and S-wave energy and the seismic moment:

$$\sigma_A = \mu (E_\alpha + E_\beta) / M_0 \quad (2.10)$$

The apparent stress is proportional to the dynamic stress drop, but does not represent an actual stress difference. For our largest rockburst,  $\sigma_A$  calculates out at 317 Pa

## 2.11 Dynamic Stress drop.

As described above, the dynamic stress drop can be estimated from  $a_{RMS}$ , the root mean square acceleration averaged over the duration of the S wave arrival as follows:

$$\sigma_{RMS} = 3.2 \rho R a_{RMS} (f_S / f_{MAX})^{1/2}$$

where  $f_S$  = S wave corner frequency on the displacement spectrum, and  
 $f_{MAX}$  = the highest frequency of acceleration reliably recorded.

If the rupture process is not complex and rupture velocity is constant, then  $\sigma_{RMS}$  and  $\Delta\sigma$  should be similar in magnitude. For the largest rockburst in our study,  $\sigma_{RMS}$  calculates to be 1.1 Mpa, less than half of the static stress drop,  $\Delta\sigma$ , suggesting that asperities along the fault plane were important in this event.

## 2.12 Fault Displacement.

The average slip across the fault plane is useful for source characterization. For the Brune Model, the average displacement  $u$  is calculated using the definition of seismic moment rearranged:

$$u = M_0 / (\mu \pi r_0^2) \quad (2.12)$$

For the largest rockburst in our data set, the average slip across the fault was found to be 5 mm.

### Number of events in 1/2 hour periods

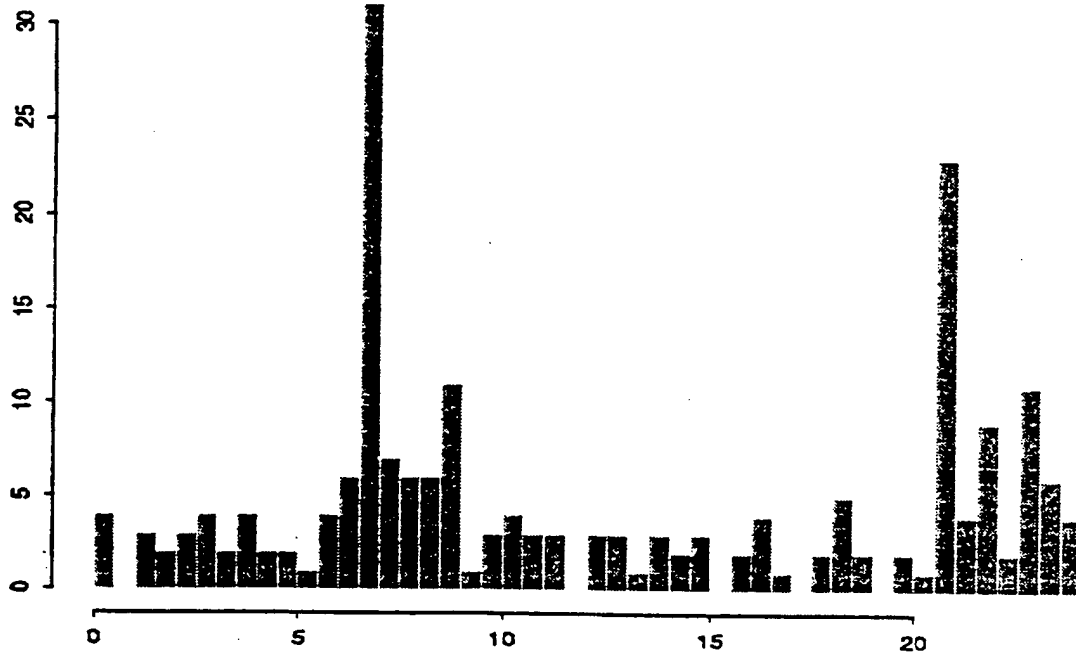


Figure 11. The average day at the Lucky Friday Mine. Although most events occur at blasting times, events can occur at any time of day.

#### 2.13 Fault Plane Solutions -- Moment Tensor Inversion.

The largest rockburst (Figure 10) analyzed in this study yielded seismograms with a moment tensor solution involving a significant volumetric component. The moment tensor was decomposed into isotropic and deviatoric components from which the volumetric closure and total shear deformation were estimated for comparison with in-mine coseismic damage. The magnitude 3.1 burst occurred 7.5 hours after routine daily blasting in the mine (Figure 11). The event represented the result of deep underground mining combined with sliding on nearby bedding planes or faults. The implosional characteristic may prove to be a useful parameter for fingerprinting seismic events from deep hardrock mines.

The moment tensor of the rock burst was estimated in the far field using a linear inversion method in the time domain:

$$\mathbf{U} = \mathbf{G} \mathbf{m} \quad (2.13)$$

where

- $\mathbf{U}$  =  $n$  sampled observations of ground displacement at the various stations,
- $\mathbf{G}$  = an  $n \times 6$  matrix containing the Green's functions calculated by the appropriate algorithm and earth model, and
- $\mathbf{m}$  = ( $M_{11}$ ,  $M_{12}$ ,  $M_{22}$ ,  $M_{13}$ ,  $M_{23}$ ,  $M_{33}$ ), a vector containing the six moment tensor elements to be determined (Gibowicz and Kijko, 1994).

Green's functions were formulated in a simple manner using the displacement vectors for far field P, SV, and SH wave radiation (Pujol and Herrmann, 1990) at each of the five stations. A synchronous source in the form of a step function was used to estimate displacements. Based on observations by Stickney and Sprenke (1993), we assumed a isotropic and homogeneous velocity model with a P-wave velocity of 5.74 km/s, and S-wave velocity of 3.47 km/s. A density of 2.7 was assumed for the metasedimentary rocks in the mine area.

The far-field contribution of a point source to P or S wave particle displacement at a given location is given by:

$$u_c(t) = 4 \pi \rho c^3 R^c R^{-1} M_0'(t-R/c) \quad (2.14)$$

where  $u_c$  is displacement of the P, SV, or SH wave,  $R^c$  is the radiation pattern, and  $M_0'(t)$  is the time history of the seismic moment  $M_0$ . Following McGarr (1991), the time history of each moment tensor component is assumed to be:

$$M_0'(t) = \begin{cases} M_0 f (1 - \cos 2 \pi f t) & \text{for } 0 \leq t \leq 1/f \\ 0 & \text{otherwise} \end{cases} \quad (2.15)$$

where  $f$  is the inverse of the displacement pulse duration. Because we measure the peak displacement of the three waves, we use  $M_0'(t) = 2 M_0 f$  at the time of the maximum pulse displacement and  $M_0'(t) = 0$  otherwise.

Figure 12 shows Greens functions for the study area centered on the Lucky Friday mine. For the simulation, the surface is considered flat. The nature of P, SV and SH displacement can be readily seen in comparison with the nine couples that compose the seismic moment tensor (Figure 13).

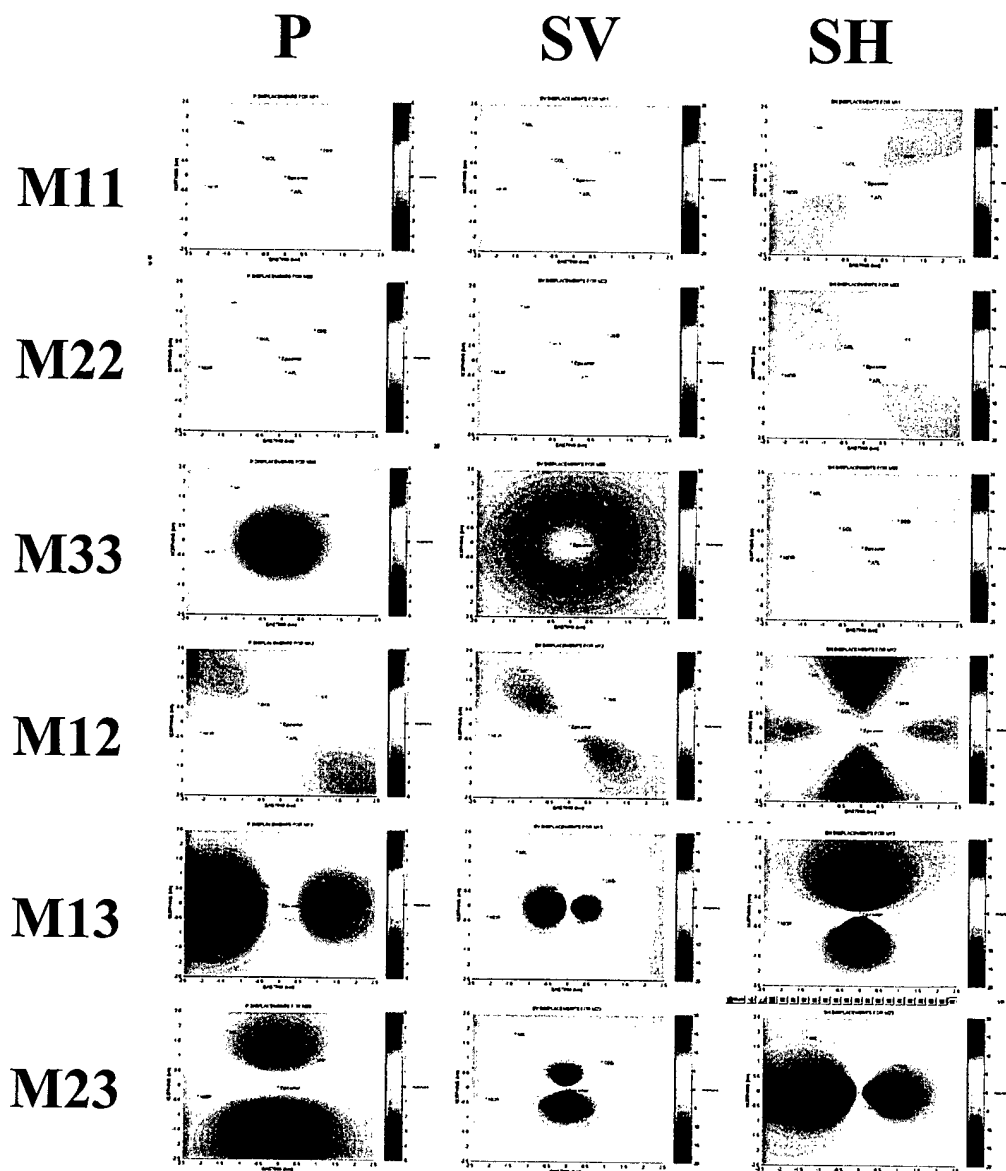


Figure 12. Greens functions for the study area. The simulated M3.1 hypocenter is at a depth of 1750 m in the center of the mine area. The accelerometer stations are indicated. The red areas are compressional, the blue, dilatational.

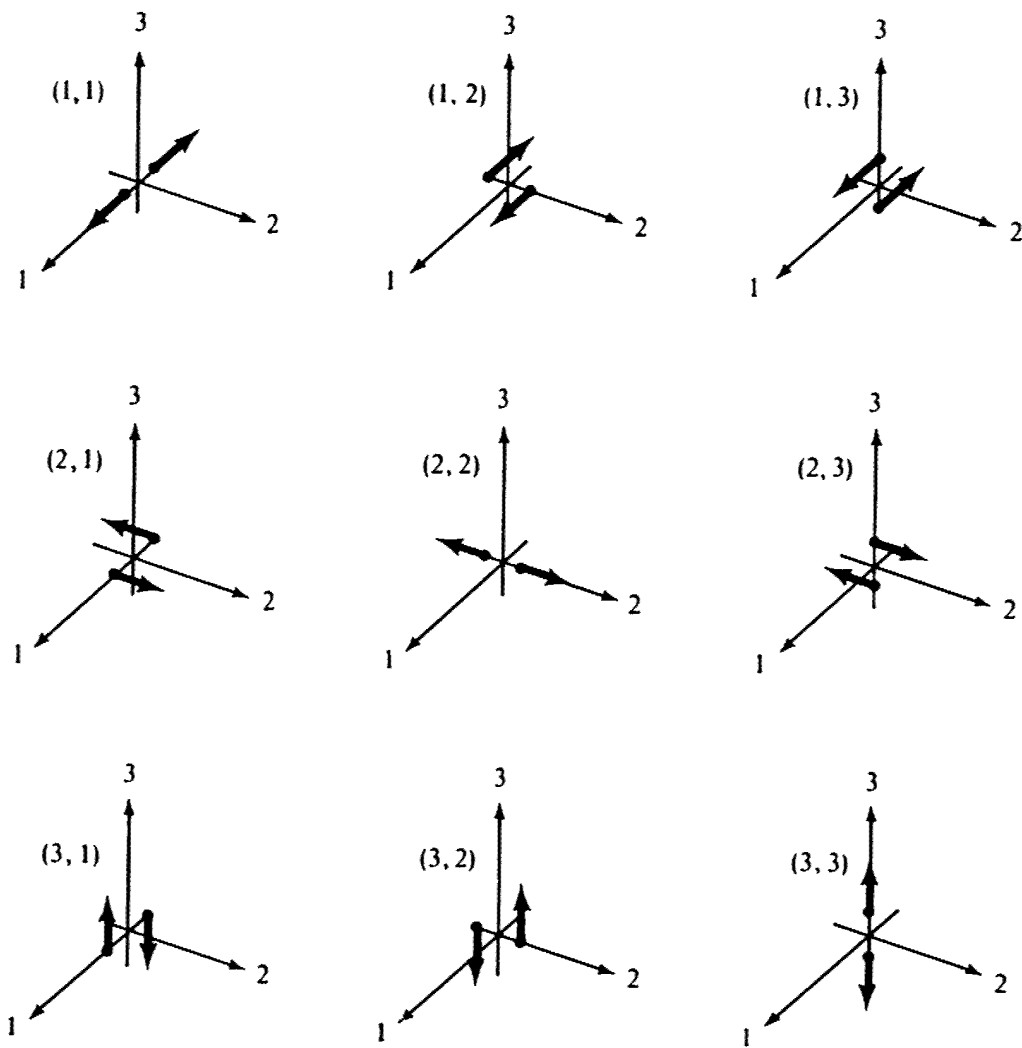
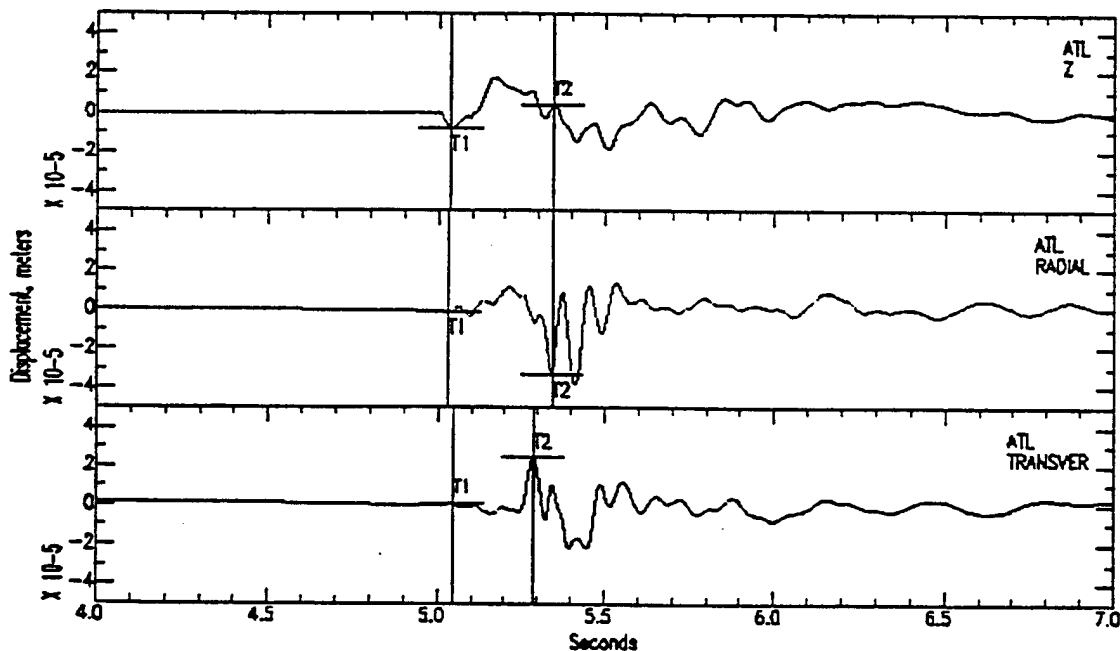


Figure 13. The nine couples composing the seismic moment tensor (Aki and Richards, 1980).

## 2.14 Analysis of Near-Field Data.

For this project, we investigated the seismic signals from a damaging rock burst in the Lucky Friday Mine. The local magnitude of the event was 3.1 as measured at Butte, Montana. It was recorded on the Montana and Washington region networks. Predominantly dilatational first motions for this event from our five local stations and several regional stations suggested that this event had an implosional component. To test this hypothesis, we performed a moment tensor inversion using the signals from five strong motion accelerometers that were deployed in the immediate area of the mine (Figure 9).

The seismic signals used in this experiment were collected as part of a local network deployment of five strong motion accelerometers and one broadband seismometer from 6-11-98 to 9-2-98 in the immediate vicinity of the Lucky Friday Mine. The damaging rock burst was the largest seismic event recorded in that period. One accelerometer was located in an abandoned adit; the remaining stations were surface stations. The data used were the maximum displacement amplitudes of the P, SV, and SH waves as recorded at the five three-component strong motion stations surrounding the site (Figures 14-18). Linear trends in the records were identified and removed. Because of their clarity, the records were not filtered. The amplitudes of the P, SH, and SV phases were measured at each of the five stations, and corrected for the free surface effect. The source location was provided by the in-mine geophone array operated by the mine.



**Figure 14.** Displacement amplitudes at ATL for the largest burst recorded in this study. The P and S picks are also shown. See Figure 9 for locations of the stations.

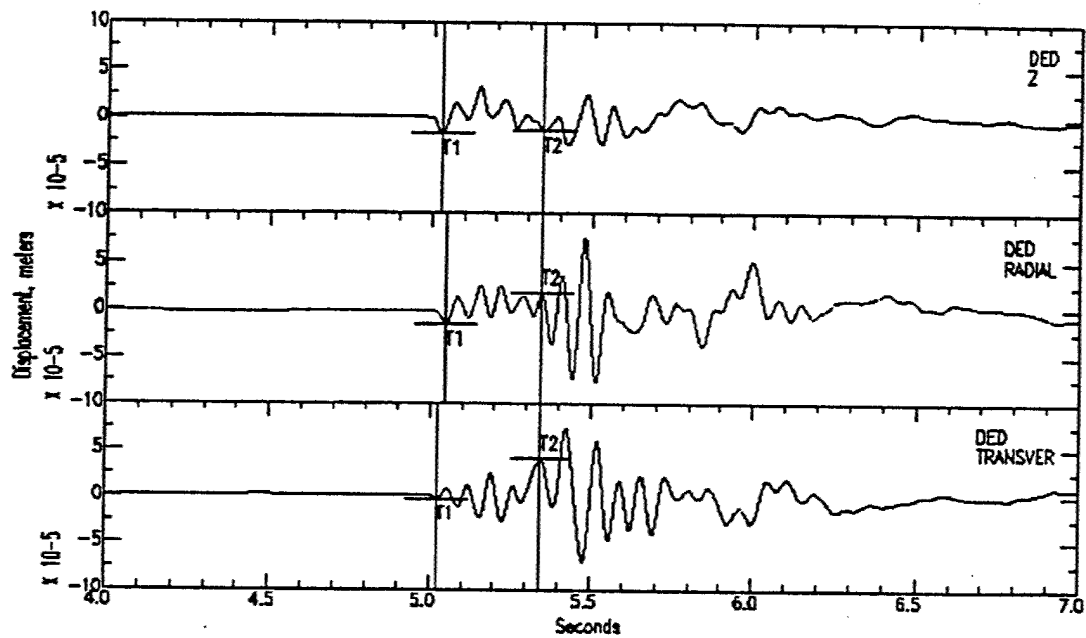


**Figure 15.** Displacement amplitudes at DED for the largest burst recorded in this study. The P and S picks are also shown. See Figure 9 for locations of the stations.

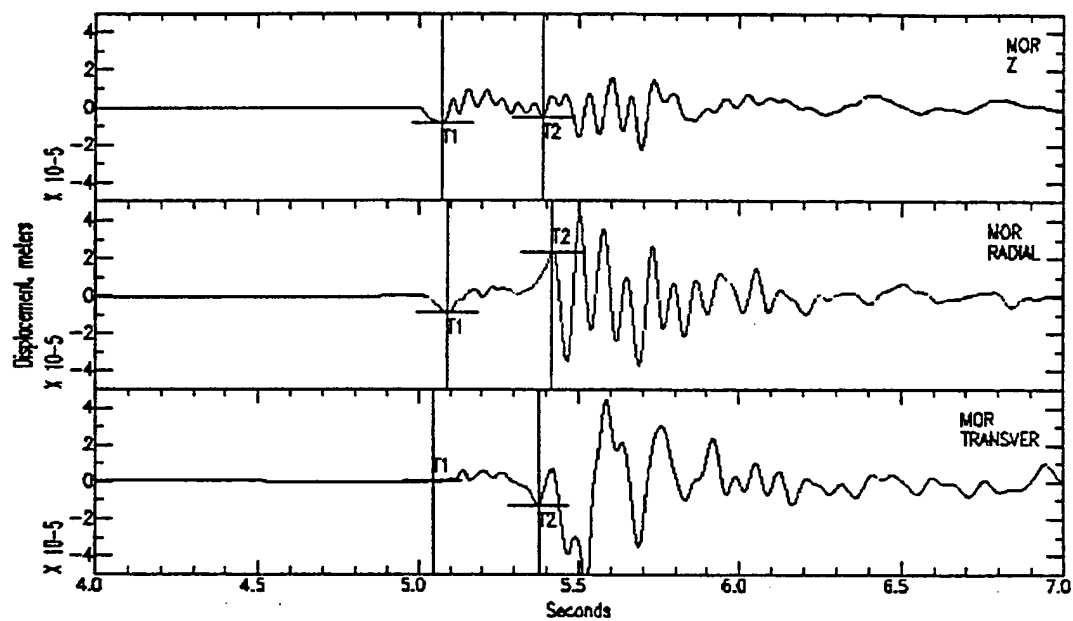


**Figure 16. Displacement amplitudes at MOR for the largest burst recorded in this study. The P and S picks are also shown. See Figure 9 for locations of the stations.**



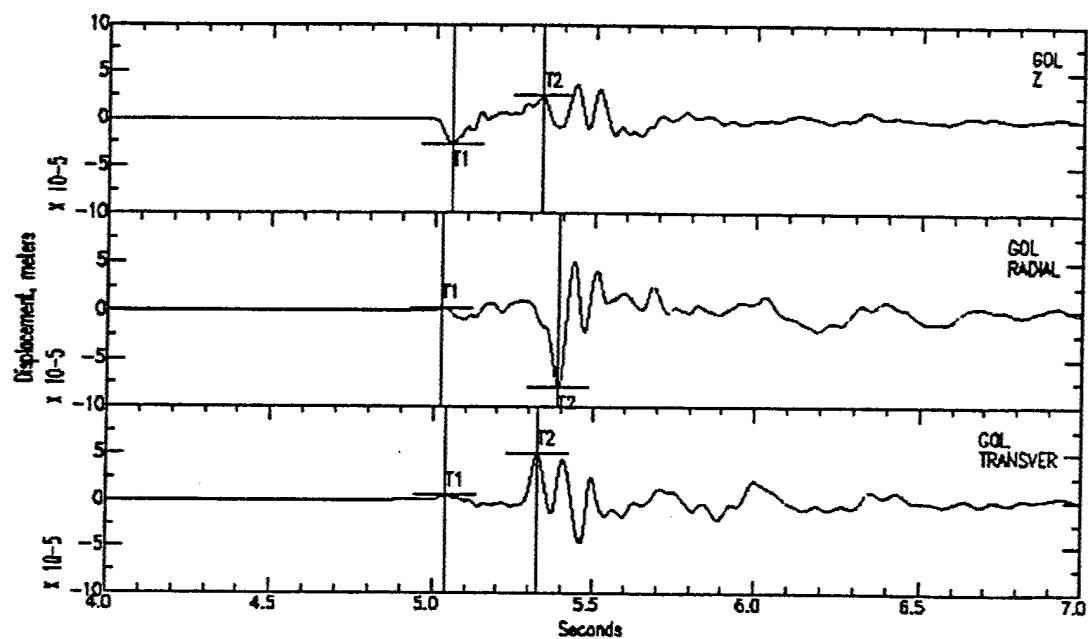


**Figure 17.** Displacement amplitudes at GOL for the largest burst recorded in this study. The P and S picks are also shown. See Figure 9 for locations of the stations.

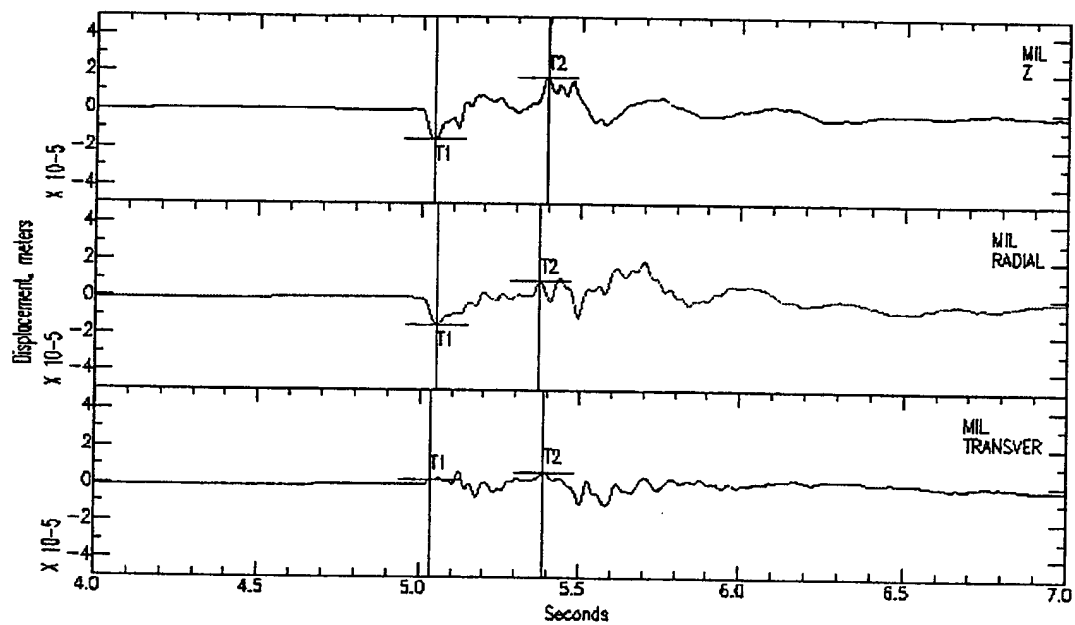
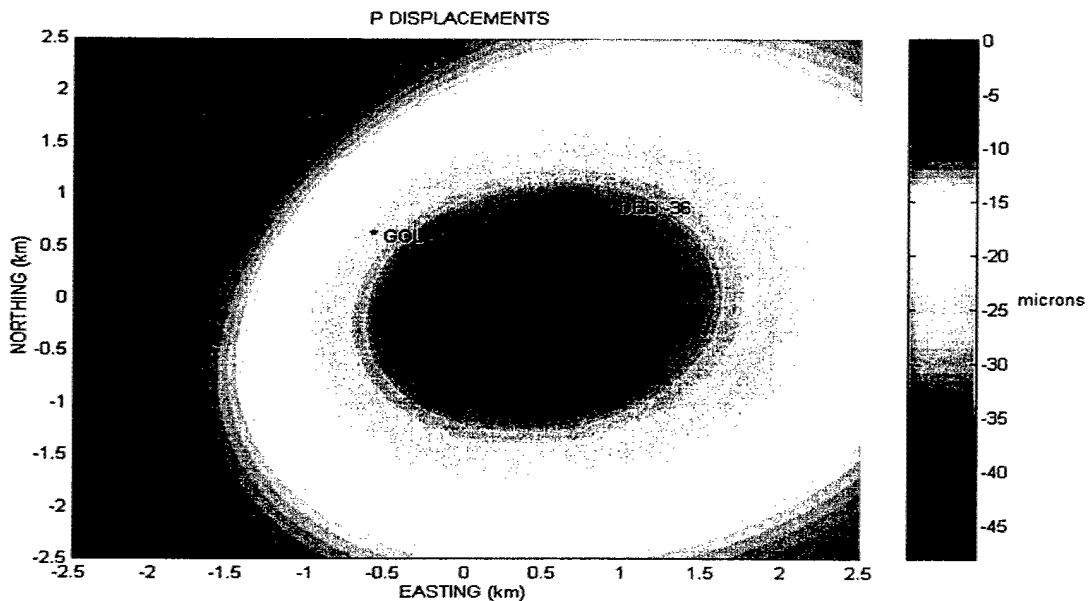


Figure 18. Displacement amplitudes at MIL for the largest burst recorded in this study. The P and S picks are also shown. See Figure 9 for locations of the stations.

To estimate the moment tensor elements, we followed a least squares procedure outlined by McGarr (1992). We found the following moment tensor solution:

$$M = \begin{bmatrix} -0.0743 & -0.1041 & -0.3102 \\ & -0.1373 & -0.0738 \\ & & -1.0000 \end{bmatrix} \times 5.03 \times 10^{13} \text{ N-m} \quad (2.16)$$

The plots of surface displacements for this solution in the mine area show that the mechanism is an excellent example of a shear-implosional failure. The P displacements (Figure 19) are dominated by the large negative M33 tensor component. This results in dilatational first-motions on all seismic stations. The implosional nature of the rock burst is clearly evident on this figure. The stereographic projection of the P first motions (Figure 20) shows all dilations except for a small region of compressive first motions. The SV and SH displacements (Figures 21 and 22) appear to be dominated by a negative M13 component, suggesting slip on faults that cut through the mine area. The shear nature of the event is very evident on the S displacements.



**Figure 19.** The P displacements for the largest burst observed the shown on a plan view of the mine area. The implosional (negative M33) nature of the event is clearly evident.

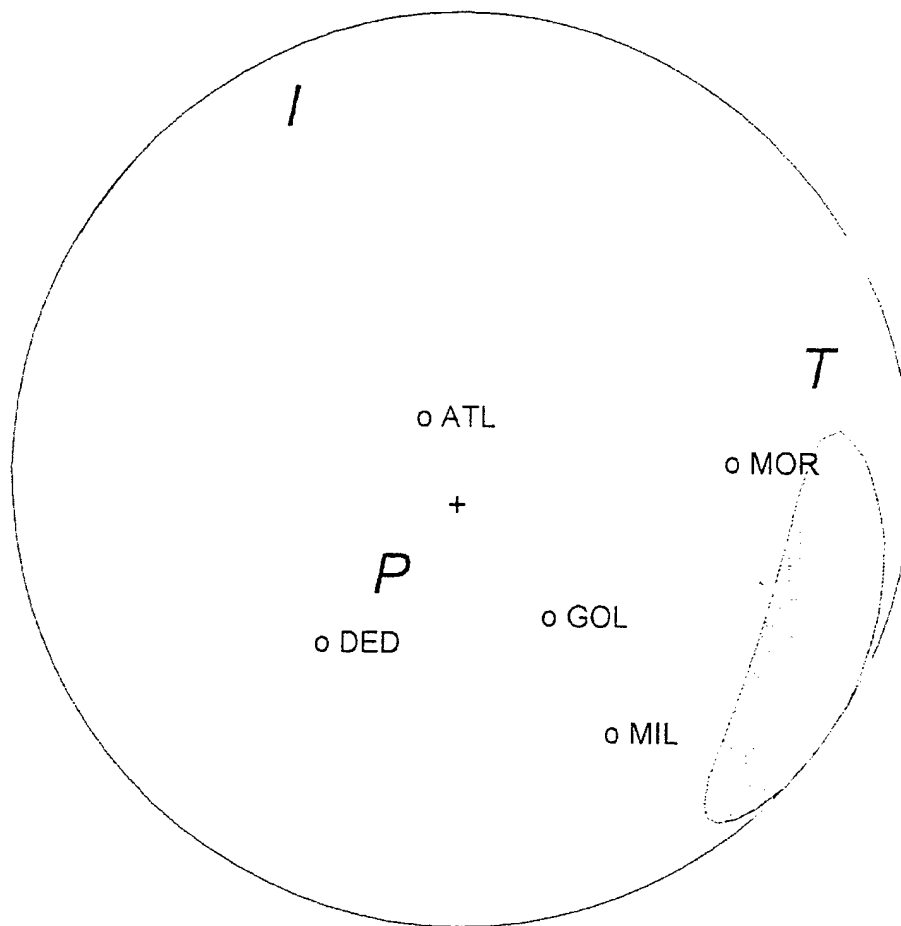
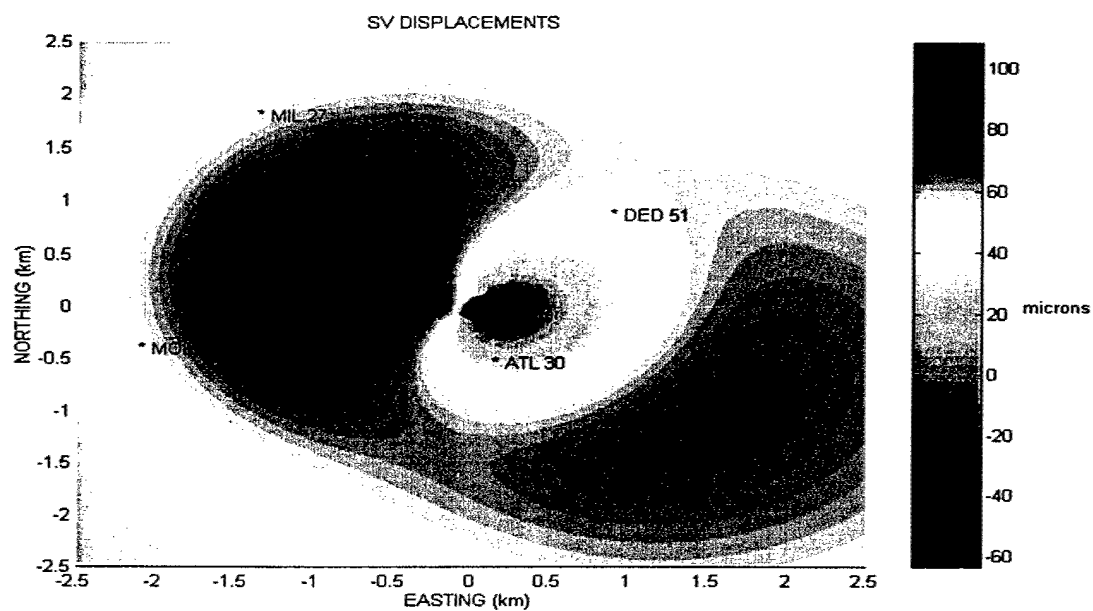


Figure 20. The P displacement polarity plotted on the lower hemisphere of an equal-area stereographic projection.



**Figure 21. The SV displacements for the largest burst observed shown on a plan view of the mine area. The shear (negative M13) nature of the event is evident.**

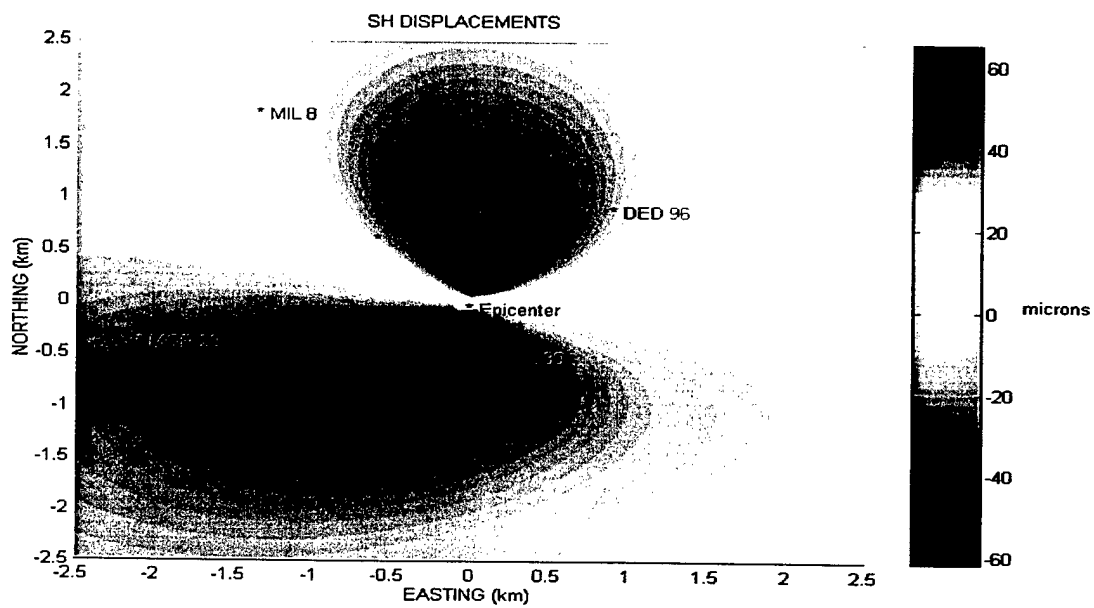


Figure 22. The SH displacements for the largest burst observed shown on a plan view of the mine area. The shear (negative M13) nature of the event is apparent.

To further interpret the moment tensor elements, we first followed the procedure outlined by McGarr (1992) in his study of South African rock bursts. The amount of coseismic closure ( $\Delta V$ ) due to the implosion can be computed using the trace of the moment tensor along with the estimated elastic properties of the metasedimentary quartzites in the mine area:

$$\Delta V = \text{tr}(M_{ij}) / (3\lambda + 2\mu) = (-6.09 \times 10^{13} \text{ N-m}) / (1.63 \times 10^{11} \text{ Pa}) \quad (2.17)$$

or  $= -379 \text{ m}^3$  of coseismic volume change.

To compute the shear deformation, the moment tensor is first diagonalized:

$$M(\text{diag}) = \begin{vmatrix} 0.0536 & 0 & 0 \\ 0 & -0.1603 & 0 \\ 0 & 0 & -1.1049 \end{vmatrix} \times 5.03 \times 10^{13} \text{ N-m} \quad (2.18)$$

The Eigenvectors, representing directions of the seismic P, I, and T axes, respectively are:

$$\begin{pmatrix} 0.8887 & 0.3499 & -0.2963 \\ -0.3942 & 0.9131 & -0.1043 \\ -0.2340 & -0.2095 & -0.9494 \end{pmatrix} \quad (2.19)$$

The deviatoric component is estimated by subtracting the volumetric component:

$$M(\text{dev}) = M(\text{diag}) - 1/3 \text{ tr}(M_{ij}) \quad (2.20)$$

$$M(\text{dev}) = \begin{vmatrix} 0.4566 & 0 & 0 \\ 0 & 0.2427 & 0 \\ 0 & 0 & -0.7019 \end{vmatrix} \times 5.03 \times 10^{13} \text{ N-m}$$

Decomposing into a major and minor double-couple:

$$M(\text{dev}) = \begin{vmatrix} 0.70 & & \\ & 0 & \\ & & -0.70 \end{vmatrix} + \begin{vmatrix} -0.24 & & \\ & 0.24 & \\ & & 0 \end{vmatrix} \quad (2.21)$$

For the major double-couple, the P axis is vertical and the T axes is east. For the minor double couple, the P axis is east and the T axis is north.. These agree well with the dominant east-northeasterly direction of tectonic extension in the area.

The total shear deformation:

$$\Sigma AD = \{M1(dev) + M2(dev)\} / \mu$$

$$\text{or } \Sigma AD = [(0.46+0.24) \times 5.03 \times 10^{13} \text{ N-m}] / (3.76 \times 10^{10} \text{ Pa}) \quad (2.22)$$

$$\Sigma AD = 909 \text{ m}^3, \text{ 2.4 times larger than the volumetric reduction.}$$

An alternative approach to interpret the moment tensor solution is to apply a crack closure (CC) mechanism. This is the negative of the tension crack (TC) suggested by Aki and Richards (1980):

$$M(\text{crack}) = \begin{vmatrix} vx & 0 & 0 \\ 0 & vx & 0 \\ 0 & 0 & x \end{vmatrix} \quad (2.23)$$

where  $v = \lambda / (\lambda + 2\mu) \approx 1/3$ ,  $x = (\lambda + 2\mu) \Delta V$ , and  $M(\text{crack})$  is the moment tensor of a crack with change in volume  $\Delta V = u A$ , where  $u$  is the crack closure displacement and  $A$  is the area of the crack.

To implement this interpretation, we begin with the diagonalized moment tensor:

$$M(\text{diag}) = \begin{vmatrix} M1 & 0 & 0 \\ 0 & M2 & 0 \\ 0 & 0 & M3 \end{vmatrix} \quad (2.24)$$

We attempt a decomposition as follows to break the diagonalized moment tensor into a crack closure, a double dipole  $M(\text{dd})$ , and an error term  $M(\epsilon)$ .

$$M(\text{diag}) = M(\text{crack}) + M(\text{dd}) + M(\epsilon) \quad (2.25)$$

$M(\text{dd})$  can take three forms, depending on the orientation of the double dipole:

$$\begin{vmatrix} M' & 0 & 0 \\ 0 & -M' & 0 \\ 0 & 0 & 0 \end{vmatrix} \text{ or } \begin{vmatrix} 0 & 0 & 0 \\ 0 & M' & 0 \\ 0 & 0 & -M' \end{vmatrix} \text{ or } \begin{vmatrix} -M' & 0 & 0 \\ 0 & 0 & 0 \\ 0 & 0 & M' \end{vmatrix} \quad (2.26)$$

For our data, the third form above gave the best-fit result. We obtain three simultaneous equations.

$$\begin{aligned} M1 &= x/3 - M' \\ M2 &= x/3 \\ M3 &= x + M' \end{aligned} \quad (2.27)$$



The least square solution to these equations yields an estimate of  $x$  and  $M'$  and the error  $M(\epsilon)$ .

For our data, we obtain  $x = -0.7546 \times 5.03 \times 10^{13}$  N-m and  $M' = 0.3276 \times 5.03 \times 10^{13}$  N-m.

$$M(\text{crack}) = \begin{vmatrix} -0.2513 & 0 & 0 \\ 0 & -0.2515 & 0 \\ 0 & 0 & -0.7546 \end{vmatrix} \times 5.03 \times 10^{13} \text{ N-m} \quad (2.28)$$

$$M(\text{dc}) = \begin{vmatrix} 0.3276 & 0 & 0 \\ 0 & 0 & 0 \\ 0 & 0 & -0.3276 \end{vmatrix} \times 5.03 \times 10^{13} \text{ N-m} \quad (2.29)$$

$$M(\epsilon) = \begin{vmatrix} 0.0227 & 0 & 0 \\ 0 & -0.0912 & 0 \\ 0 & 0 & 0.0227 \end{vmatrix} \times 5.03 \times 10^{13} \text{ N-m} \quad (2.30)$$

This result, with an overall RMS error of  $0.0557 \times 5.03 \times 10^{13}$  N-m, is the best fit of the three cases considered for the double couple. The other two cases produced errors 4 to 5 times larger. Comparing with the Eigenvectors above, this double couple has an east-northeast T-axis and a near vertical P-axis. This solution is consistent with the regional stress direction, and it, like the McGarr model, produces the anticipated normal slip predicted by the negative M13 component of the stress tensor solution.

The volume reduction in the mine  $\Delta V = x/(\lambda + 2\mu)$  works out to be  $-420 \text{ m}^3$ . The shear deformation due to the double couple  $\Sigma AD = M'/\mu$  is as:

$$\Sigma AD = [(0.3276) \times 5.03 \times 10^{13} \text{ N-m}] / (3.76 \times 10^{10} \text{ Pa}) \quad (2.31)$$

$$\Sigma AD = 350 \text{ m}^3, \text{ or about 83\% of the volumetric reduction.}$$

It is interesting to note that the  $M(\epsilon)$  error term from the least squares fit is similar in form to a compensated linear vector dipole (CVLD):

$$M(\text{CVLD}) = \begin{vmatrix} -x'/2 & 0 & 0 \\ 0 & -x' & 0 \\ 0 & 0 & -x'/2 \end{vmatrix} \quad (2.32)$$

except that our result appears to have one dipole of strength 4 rather than strength 2 relative to the others. At any rate the  $M(\epsilon)$  tensor is negligible in our result.

## 2.15 A Template for Shear-Implosional Rockbursts.

The moment tensor estimates for the rock burst analyzed here were found to be dominated by negative diagonal components, indicating a dominantly implosional source. However, the source is not completely isotropic. Our results are similar to those obtained for a group of events studied by McGarr (1992) from deep hard rock mining districts in South Africa, suggesting that implosional events may be characteristic of a type of event that may fingerprint such mines for CTBT purposes. Further work needs to be done to evaluate the effect of such implosional events at distances useful for treaty verification monitoring.

Regional waveforms were obtained for nearby earthquakes and explosions that have occurred in the region (Figure 23) and for the larger events analyzed in this study (Figure 24). These data were used in the second phase of this contract to evaluate the ability to discriminate between such events and shear- or implosion-dominated mine-induced events using regional waveforms.

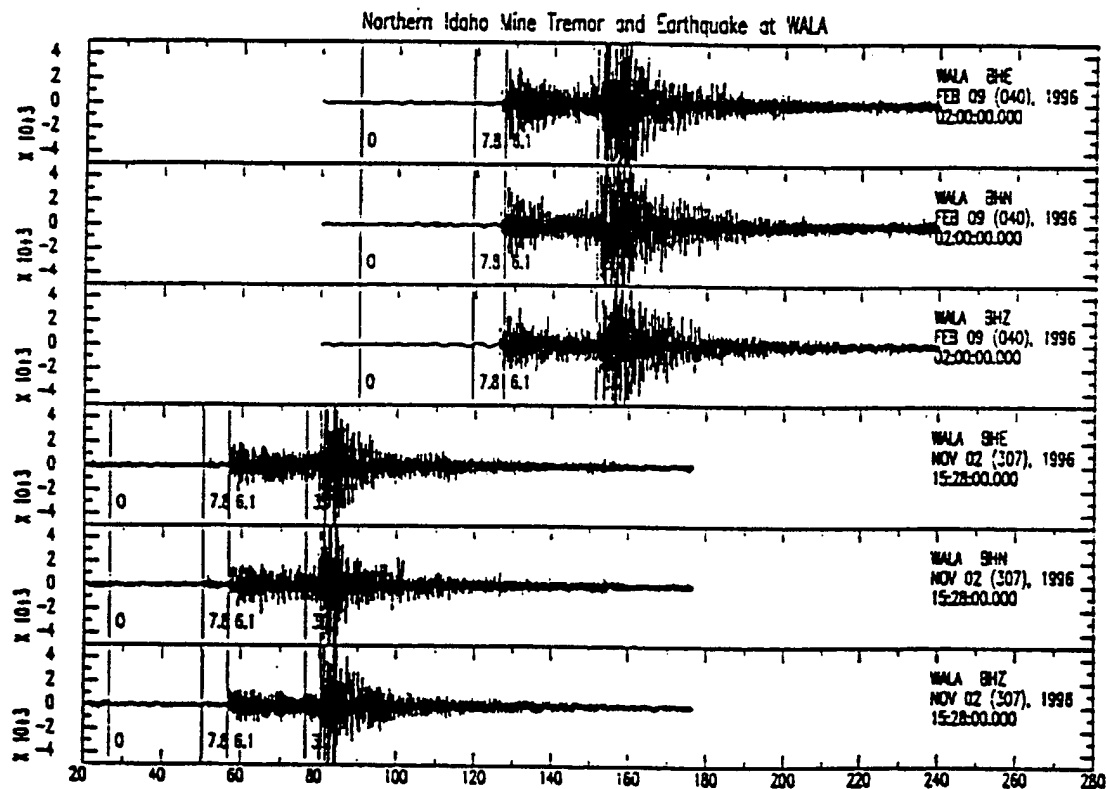
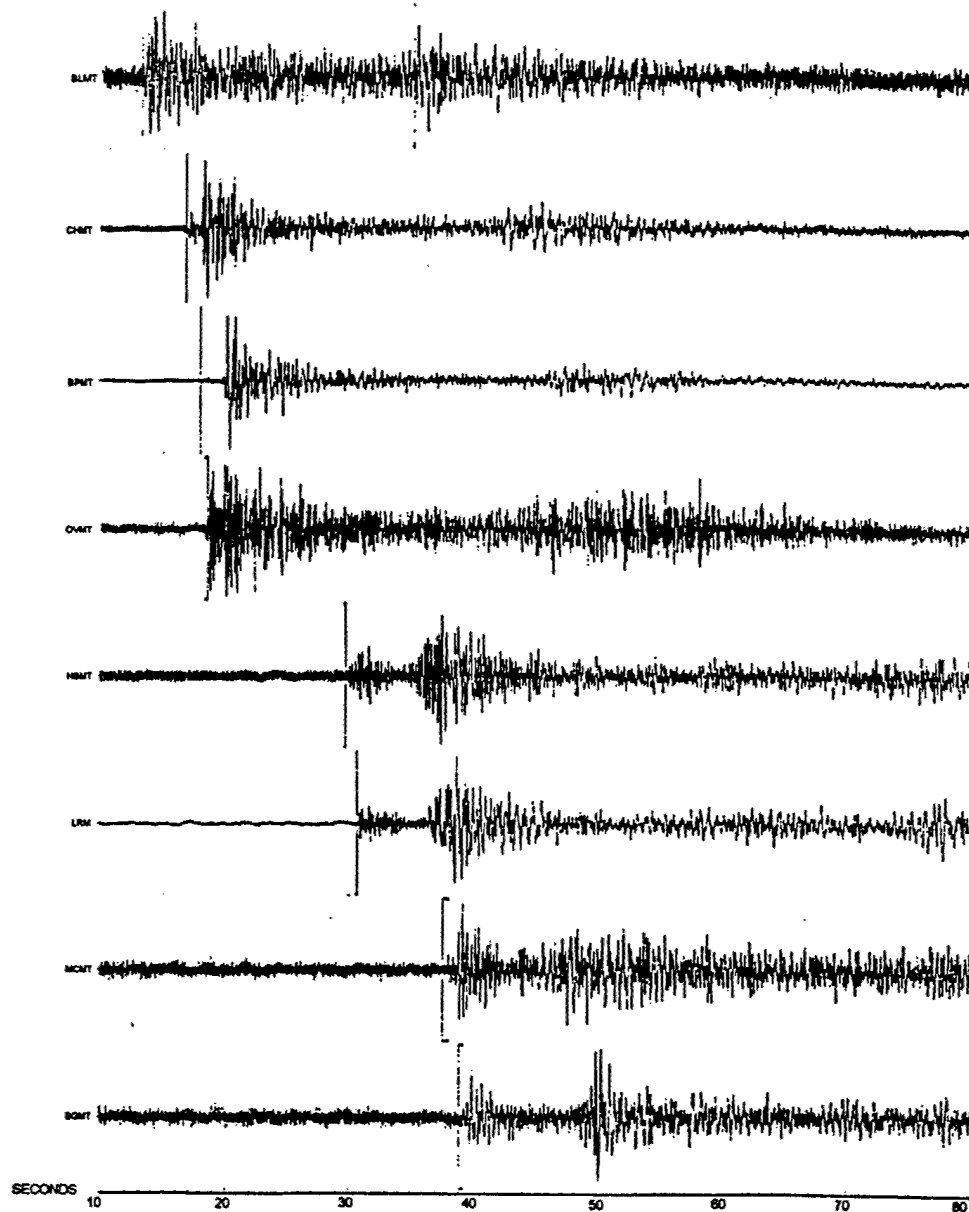


Figure 23. Waveforms at CSN seismic station WALA from a 3.6 mine tremor on Feb. 9, 1996 (upper) and from a recent northern Idaho earthquake (lower). Approximate group velocities of 7.8, 6.1, and 3.7 km/s are shown.



**Figure 24. Waveforms recorded at regional distances for the largest burst observed during this study.**

The key to fingerprinting many of the rock bursts from deep underground mines such as those in the Silver Valley is to make use of the implosional component of the bursts that seems to be associated with the majority of the bursts and the consequent lack of Love waves associated with such sources. For example, Pechman et al. (1995) have shown that five broadband stations at distances from 300 and 1000 km were sufficient to resolve the focal mechanism and seismic moment of the implosional  $M_L 5.1$  Trona Mine event. In the present study, we have shown that the source characteristics of the rockbursts in the Coeur d'Alene Mining District are similar to those of the Trona Mine event. Thus the methods used to characterize the Trona Mine event are also applicable to deeper underground events as well.

The Trona Mine event was characterized by modeling its long period waveforms using a regional velocity model in conjunction with methodology as described by Walter (1993). The seismograms evaluated were instrument-corrected displacement records band passed filtered from 20 to 40 seconds. The seismograms showed little long period Pnl or Love wave amplitude. Pnl and Love wave energy is characteristic of earthquakes, but not explosions or mine collapses. Sufficient broadband stations are necessary, however, to ensure that azimuthal coverage is sufficient to avoid Love Wave nodes at particular azimuths.

The horizontal tension crack model appears to at least partially characterize both shallow and deep mine collapses. The collapsing crack model produces all dilatational first arrivals, and for the case of the Trona Mine events, fits the waveforms at distant stations better than a pure implosional model or an earthquake model. For the shear implosional mechanism apparent in the Coeur d'Alene District events, a combination of the collapsing crack model and a double couple needs to be employed to better fit the waveforms at regional distances. Figure 24 compares a rock burst and earthquake record from north Idaho. Both events clearly have well developed Love waves, so a simple implosional or collapsing crack model will fail to adequately model the waveforms. A shear implosional source would have to be employed instead.

Seismic events related to mining are commonly thought to be of two distinct types. Type 1 events are caused by implosion; type 2 are tectonic events involving fault slip triggered somehow by mining. The deep underground rock bursts in the Silver valley appear to be a hybrid event involving both implosion and shear along failure planes.

### SECTION 3 REFERENCES

Aki, K., and P.G. Richards, 1980, Quantitative Seismology, Freeman, San Francisco. (UNCLASSIFIED)

Banfill, R., 1996, PC-SUDS utilities: A collection of tools for routine processing of seismic data stored in the Seismic Unified Data System for DOS, version 2.5; Small Systems Support, Big Water, Utah, 178 p.(UNCLASSIFIED)

Bennett, T.J., M.E. Marshall, K.L. McLaughlin, B.W. Barker, and J.R. Murphy. 1995. Seismic characteristics and mechanisms of rockbursts. In Proceedings of the 17th Annual Seismic Research Symposium on Monitoring a Comprehensive Test Ban Treaty, 12-15 September 1995. Edited by J.F. Lewkowicz, J.M. McPhetres, and D.T. Reiter. 1995. PL-TR-95-2108, Environmental Research Papers, No. 1173, p. 542. (UNCLASSIFIED)

Bennett, T.J., M.E. Marshall, K.L. McLaughlin, B.W. Barker, and J.R. Murphy. 1996. Seismic Investigations of rockbursts. In Proceedings of the 18th Annual Seismic Research Symposium on Monitoring a Comprehensive Test Ban Treaty. Edited by J.F. Lewkowicz, J.M. McPhetres, and D.T. Reiter. PL-TR-96-2153. (UNCLASSIFIED)

Blake, W., Rock preconditioning as a seismic control measure in mines, in rockbursts and Seismicity in Mines, Symp. Ser. vol. 6, edited by E.H. Wainwright, pp. 225-234, South African Institute of Mining and Metallurgy, Johannesburg, Kelvin House, Johannesburg, 1984. (UNCLASSIFIED)

Blake, W., and D.J. Cuvelier, Developing reinforcement requirements for rockburst conditions at Hecla's Lucky Friday Mine, in Proceedings of 2nd International Congress on Rockbursts and Seismicity in Mines, Minneapolis, Balkema Publishers, Rotterdam, pp. 589-598, 1990. (UNCLASSIFIED)

Gane, P.G., P. Seligman, and J.H. Stephen, Focal depths of Witwatersrand tremors, Bull. Seismol. Soc. Am., 42, 239-250, 1952. (UNCLASSIFIED)

Gibowicz, S.J., Harjes, H.-P., and Schafer, M., 1990. Source parameters of seismic events at Heinrich Robert mine, Ruhr basin, Federal Republic of Germany: Evidence for nondouble-couple events. BSSA, 80, 88-109. (UNCLASSIFIED)

Gibowicz, S.J. and A. Kijko, 1994. An Introduction to Mining Seismology. Academic Press, Inc., San Diego, 399 pp. (UNCLASSIFIED)

Guth, P.L., 1987. MicroNet, Interactive Schmidt and Wulff nets for the MS-DOS PC. Department of Geoscience, University of Nevada, Las Vegas, NV. (UNCLASSIFIED)

Heuze, F.E., 1994. Rockbursts as opportunities for the concealment of nuclear tests? UCRL-ID-116123. Lawrence Livermore National Laboratory, January, 7 pp. (UNCLASSIFIED)

Hobbs, S.W., A.B. Griggs, R.E. Wallace, and A.B. Campbell, Geological Survey, Coeur d'Alene district, Shoshone County, Idaho, U.S. Geol. Surv. Prof. Pap. 478, 139 pp., 1965. (UNCLASSIFIED)

Jung, S.J., P.B. Lourence, and K.F. Sprenke, 1995. Fault plane solutions of mining-induced seismicity, Lucky Friday Mine, northern Idaho. Exploration Mining Geology, 4, 65-71. (UNCLASSIFIED)

Kozak, J., and J. Sileny, Seismic events with non-shear component, I, Shallow earthquakes with possible tensile source component, Pure Appl. Geophys., 123, 1-15, 1985. (UNCLASSIFIED)

Lee, W. H. K., and C.M. Valdes, HYPO71PC: A personal computer version of the HYPO71 earthquake location program, U.S. Geol. Surv. Open-File Rep. 85-749, 43 pp., 1985. (UNCLASSIFIED)

Lee, W.H.K. and Lahr, J.C., 1975, HYPO71 (revised): A computer program for determining hypocenter magnitude, and first motion pattern of local earthquakes; U.S. Geological Survey Open-File Report 75-311, 113 p. (UNCLASSIFIED)

McGarr, A., Violent deformation of rock near deep-level, tabular excavations-seismic events, Bull. Seismol. Soc. Am., 61, 1453- 1466, 1971. (UNCLASSIFIED)

McGarr, A., Some applications of seismic source mechanism studies to assessing underground hazard, in Rockbursts and Seismicity in Mines, Symp. Ser. vol. 6, edited by N.C. Gay and E.H. Wainwright, pp. 147-152, South African Institute of Mining and Metallurgy, Johannesburg, Kelvin House, Johannesburg, 1984. (UNCLASSIFIED)

McGarr, A., 1992. Moment tensors of ten Witwatersrand mine tremors, PAGEOPH, 139, 781-800. (UNCLASSIFIED)

McGarr, A., S.M. Spottiswoode, and N.C. Gay, Relationship of mine tremors to induced stresses and to rock properties in the focal region, Bull. Seismol. Soc. Am., 65, 981-993, 1975. (UNCLASSIFIED)

Mckenzie, D.P., 1969. The relation between fault plane solutions for earthquakes and the directions of the principal stresses. Bulletin of the Seismological Society of America, 59, p. 591- 601. (UNCLASSIFIED)

Ortlepp, D.A., 1983. The mechanism and control of rockbursts. In Rock Mechanics in Mining Practice. Edited by S. Budavari. The South African Institute of Mining and Metallurgy. Johannesburg, p. 257-281. (UNCLASSIFIED)

Pechmann, J.C., W.R. Walter, S.J. Nava, and W.J. Arabasz, 1995. The February 3, 1995, ML 5.1 seismic event in the Trona Mining District of southwestern Wyoming, *Seis. Res. Let.*, 66, 25-34. (UNCLASSIFIED)

Pujol, J. and R.B. Herrmann, 1990. A students guide to point sources in homogeneous media. *Seismol. Res. Letters*, 61, 209-224. (UNCLASSIFIED)

Reasenber, P. A., and D. Oppenheimer, FPFIT, FPLOT and FPPAGE: FORTRAN computer programs for calculating and displaying earthquake fault plane solutions, U.S. Geol. Surv. Open-File Rep. 85-739, 109 pp., 1985. (UNCLASSIFIED)

Rudajev, V., and S. Sileny, Seismic events with non-shear component, II. Rockbursts with implosive source component, *Pure Appl. Geophys.*, 123, 17-25, 1985. (UNCLASSIFIED)

Ryder, J.A., 1988. Excess shear stress in the assessment of geologically hazardous situations. *Journal of the South African Institute of Mining and Metallurgy*, 88, p. 27-39. (UNCLASSIFIED)

Scott, D.F., 1990. Relationship of geological features to seismic events, Lucky Friday Mine, Mullan, Idaho. In *Rockbursts and Seismicity in Mines* (C. Fairhurst, ed.), 401-405, Balkema, Rotterdam. (UNCLASSIFIED)

Scott, D.F., B.C. White and T.J. Williams, 1993. Host structures for slip-induced seismicity at the Lucky Friday Mine. In *Rockbursts and Seismicity in Mines '93*. Edited by R.P Young. A.A. Balkema, Rotterdam, p.245-248. (UNCLASSIFIED)

Sileny, J., A.R. Ritsema, I. Csikos, and J. Kozak, Do some shallow earthquakes have a tensile source component?, *Pure Appl. Geophys.*, 124, 825-840, 1986. (UNCLASSIFIED)

Spottiswoode, S.M., and A. McGarr, Source parameters of tremors in a deep-level gold mine, *Bull. Seismol. Soc. Am.*, 65, 93- 112, 1975. (UNCLASSIFIED)

Sprenke, K. F., M.C. Stickney, D.A. Dodge, and W.R. Hammond, Seismicity and tectonic stress in the Coeur d'Alene Mining District, *Bull. Seismol. Soc. Am.*, 81, 1145-1156, 1991. (UNCLASSIFIED)

Sprenke, K.F., M.C. Stickney, D.A. Dodge and W.R. Hammond, 1991. Seismicity and tectonic stress in the Coeur d' Alene mining district. *Bulletin of the Seismological Society of America*, 81, p. 1145-1156. (UNCLASSIFIED)

Stickney, M.C., 1997, Seismic source zones in southwest Montana; Montana Bureau of Mines and Geology Open-File report 366, 52 p. (UNCLASSIFIED)

Stickney, M.C., 1995, Montana seismicity report for 1990; Montana Bureau of Mines and Geology Miscellaneous Contribution 16, 44 p. (UNCLASSIFIED)

Stickney, M.C. and K.F. Sprenke, 1993. Seismic events with implosional focal mechanisms in the Coeur d'Alene mining District, northern Idaho. *Journal of Geophysical Research*, 98, p. 6523-6528. (UNCLASSIFIED)

Stickney, M. C., and M.J. Bartholomew, Seismicity and late Quaternary faulting of the northern Basin and Range province, Montana and Idaho, *Bull. Seismol. Soc. Am.*, 77, 1602-1625, 1987. (UNCLASSIFIED)

Stiller, H., E. Hurtig, H. Grosser, and P. Knoll, On the nature of mining tremors, *Earthquake Pred. Res.*, 2, 57-67, 1983. (UNCLASSIFIED)

Taylor, S.R. 1994. False alarms and seismicity: An example from the Gentry Mountain Mining Region, Utah, *Bull. Seismol. Soc. Am.*, 84, 350-358. (UNCLASSIFIED)

Taylor, S.R., M.D. Denny, E.S. Vergino, and R.E. Glaser, 1989. Regional discrimination between NTS explosions and western U.S. earthquakes, *Bull. Seismol. Soc. Am.*, 79, 1142-1176, 1989. (UNCLASSIFIED)

Teisseyre, R., Some remarks on the source mechanism of rockbursts in mines and on possible source extension, *Acta Montana*, 55, 7- 14, 1980. (UNCLASSIFIED)

Tottingham, D.M., 1994, User manual for XRTP, *in* Realtime seismic data acquisition and processing, IASPEI Software Library Volume 1, Second Edition, edited by W.H.K. Lee, pp. 207-254. (UNCLASSIFIED)

Wallace, C. A., D.J. Lidke, and R.G. Schmidt, Faults of the central part of the Lewis and Clark line and fragmentation of the Late Cretaceous foreland basin in west-central Montana, *Geol. Soc. Am. Bull.*, 102, 1021-1037, 1990. (UNCLASSIFIED)

Whyatt, J.K., T.J. Williams and W. Blake, 1993. Concentration of rockburst activity and in situ stress at the Lucky Friday Mine. In *Rockbursts and Seismicity in Mines '93*. Edited by R.P. Young, A.A. Balkema, Rotterdam, pp. 135-139. (UNCLASSIFIED)



Whyatt, J.K., T.J. Williams, W. Blake, K. Sprenke, and C. Wideman, 1996. Mining-induced seismic events at the Lucky Friday Mine: Large seismic events (magnitude > 2.5), 1989- 1994. Lawrence Livermore National Laboratory B291533, 165 pp. (UNCLASSIFIED)

Williams, D.J., and W.J. Arabasz, Mining related and tectonic seismicity in the East Mountain area, Wasatch Plateau, Utah, U.S.A., Pure Appl. Geophys., 129, 345-368, 1989. (UNCLASSIFIED)

Williams, T.J., C.J. Wideman, K.F. Sprenke, J.M. Giraud, and T.L. Nichols, 1995. Comparison of data from in-mine rockburst mining systems and the North Idaho Seismic Network, Lucky Friday Mine, Mullen, Idaho. In Proceedings: Mechanics and Mitigation of Violent Failure in Coal and Hard Rock Mines, ed. by H. Maleki, P.F. Mofat, R.C. Shepshar, and R.J. Tuchman. USBM Spec. Publ. 01-95, pp. 265-281. (UNCLASSIFIED)

Wong, I.G. and A. McGarr, Implosional failure in mining-induced seismicity: a critical review, in Proceedings of 2nd International Congress on Rockbursts and Seismicity in Mines, Minneapolis, pp. 45-51, Balkema, Rotterdam, 1990. (UNCLASSIFIED)

Wong, I.G., J.R. Humphrey, J.R. Adams, and W.J. Silva, Observations of mine seismicity in the eastern Wasatch Plateau, Utah, U.S.A.: a possible case of implosional failure, Pure Appl. Geophys., 129, 369-405, 1989. (UNCLASSIFIED)

**DISTRIBUTION LIST**

**DTRA TR- 00-15**

**DEPARTMENT OF DEFENSE**

DIRECTOR  
DEFENSE INTELLIGENCE AGENCY  
BUILDING 6000, BOLLING AFB  
WASHINGTON, DC 20340 - 5100  
ATTN: DTIB

DEFENSE RESEARCH & ENGINEERING  
WASHINGTON, DC 20301- 3110  
ATTN: DDR&E, ROOM 3E808

DEFENSE TECHNICAL INFORMATION CENTER  
8725 JOHN J KINGMAN ROAD, SUITE 0944  
FORT BELVOIR, VA 22060 - 6218  
2 CYS ATTN: DTIC/ OCP

DEFENSE THREAT REDUCTION AGENCY  
8725 JOHN J KINGMAN ROAD, MS 6201  
FORT BELVOIR, VA 22060 - 6201  
ATTN: TDND, DR. A. DAINTY  
ATTN: TDPS. LTC C. JERRETT

OFFICE OF THE SECRETARY OF DEFENSE  
NUCLEAR TREATY PROGRAMS OFFICE  
1515 WILSON BOULEVARD, SUITE 720  
ARLINGTON, VA 22209  
ATTN: P. WAKEFIELD  
ATTN: DR. S. MANGINO

**DEPARTMENT OF THE ARMY**

US ARMY SMDC  
ATTN: SMDC-TC-YD  
P.O. BOX 1500  
HUNTSVILLE, AL 35807 - 3801  
ATTN: B. ANDRE

**DEPARTMENT OF THE AIR FORCE**

AIR FORCE RESEARCH LABORATORY  
29 RANDOLPH ROAD  
HANSCOM AFB, MA 01731  
ATTN: RESEARCH LIBRARY  
ATTN: VSBL, R. RAISTRICK

USAF AT USGS  
2201 SUNRISE VALLEY DRIVE MS 951  
RESTON, VA 20192  
ATTN: R. BLANDFORD  
ATTN: R. JIH

AIR FORCE TECHNICAL APPLICATIONS CTR.  
1030 S. HIGHWAY AIA  
PATRICK AFB, FL 32925 - 3002  
ATTN: CA, STINFO  
ATTN: TTR, D. CLAUTER  
ATTN: CTI, DR. B. KEMERAIT  
ATTN: TT, DR. D. RUSSELL  
ATTN: TTR, F. SCHULT  
ATTN: TTR, G. ROTHE  
ATTN: TTR, V. HSU  
ATTN: DR. B. NGUYEN  
ATTN: DR. G. WAGNER  
ATTN: DR. M. WOODS  
ATTN: DR. N. YACOUN

**DEPARTMENT OF THE NAVY**

NAVAL RESEARCH LABORATORY  
4555 OVERLOOK AVE, SW. CODE 7643  
WASHINGTON, DC 20375 - 0001  
ATTN: DR. D. BROB

**DEPARTMENT OF THE ENERGY**

NATIONAL NUCLEAR SECURITY  
ADMINISTRATION  
1000 INDEPENDENCE AVE SW  
WASHINGTON, DC 20585 - 0420  
ATTN: L. CASEY  
ATTN: M. DENNY  
ATTN: G. KIERNAN

UNIVERSITY OF CALIFORNIA  
LAWRENCE LIVERMORE NATIONAL LAB  
P.O. BOX 808  
LIVERMORE, CA 94551 - 9900  
ATTN: MS L-205, DR. D. HARRIS  
ATTN: MS L208, TECHNICAL STAFF  
ATTN: MS L205, TECHNICAL STAFF

**DISTRIBUTION LIST**  
**DTRA TR - 00- 15**

**LOS ALAMOS NATIONAL LABORATORY**

P.O. BOX 1663

LOS ALAMOS, NM 87545

ATTN: MS C335, DR. S. R. TAYLOR

ATTN: MS - D460, FRANCESCA CHAVEZ

ATTN: MS C335, TECHNICAL STAFF

ATTN: MS D460, TECHNICAL STAFF

ATTN: MS F665, TECHNICAL STAFF

ATTN: MS D408, TECHNICAL STAFF

ATTN: MS J577, TECHNICAL STAFF

ATTN: MS D443, TECHNICAL STAFF

**PACIFIC NORTHWEST NATIONAL LABORATORY**

P.O. BOX 999

1 BATTELLE BOULEVARD

RICHLAND, WA 99352

ATTN: MS P8-20, T. HEIMBIGNER

ATTN: MS K8-29, DR. N. WOGMAN

**SANDIA NATIONAL LABORATORIES**

MAIL SERVICE

P.O. BOX 5800

ALBUQUERQUE NM 87185 - 1363

ATTN: MS 1138 TECHNICAL STAFF

DEPARTMENT 6533

**OTHER GOVERNMENT**

**DEPARTMENT OF STATE**

2201 C STREET, NW

WASHINGTON, DC 20520

ATTN: R. MORROW, ROOM 5741

**NATIONAL ARCHIVES & RECORDS**

ADMINISTRATION

8601 ADELPHI ROAD, ROOM 3360

COLLEGE PARK, MD 20740 - 6001

2 CYS ATTN: USER SERVICE BRANCH

**US GEOLOGICAL SURVEY**

ADVANCED SYSTEMS CENTER

MS 562

RESTON, VA 20192

ATTN: W. LEITH

**US GEOLOGICAL SURVEY**

345 MIDDLEFIELD RD MS 977

MENLO PARK, CA 94025

ATTN: S. DETWEILER

ATTN: DR. W. MOONEY

**DIRECTORY OF OTHER (LIBRARIES AND  
UNIVERSITIES)**

**BOSTON COLLEGE**

INSTITUTE FOR SPACE RESEARCH

140 COMMONWEALTH AVENUE

CHESTNUT HILL, MA 02167

ATTN: DR. D. HARKRIDER

ATTN: B. SULLIVAN

**BROWN UNIVERSITY**

DEPARTMENT OF GEOLOGICAL SCIENCES

75 WATERMAN STREET

PROVIDENCE, RI 02912 - 1846

ATTN: PROF D. FORSYTH

**CALIFORNIA INSTITUTE OF TECHNOLOGY**

DIVISION OF GEOLOGY & PLANETARY SCIENCES

PASADENA, CA 91125

ATTN: PROF DONALD V HELMBERGER

ATTN: PROF THOMAS AHRENS

**UNIVERSITY OF CALIFORNIA - BERKELEY**

281 MCCONE HALL

BERKELEY, CA 94720 - 2599

ATTN: PROF B. ROMANOWICZ

ATTN: DR. D. DREGER

**UNIVERSITY OF CALIFORNIA - DAVIS**

DAVIS, CA 95616

ATTN: R.H. SHUMWAY, DIV

STATISTICS

**UNIVERSITY OF CALIFORNIA - SAN DIEGO**

LA JOLLA, CA 92093 - 0225

ATTN: DR. L. DEGROOT - HEDLIN

ATTN: DR. M. HEDLIN

ATTN: PROF F. VERNON

ATTN: PROF. J. ORCUTT

ATTN: DR. G. D'SPAIN

DISTRIBUTION LIST  
DTRA TR - 00 - 15

UNIVERSITY OF CALIFORNIA - SANTA CRUZ  
INSTITUTE OF TECTONICS  
SANTA CRUZ, CA 95064  
ATTN: DR. R.S. WU  
ATTN: PROF T. LAY

UNIVERSITY OF COLORADO - BOULDER  
DEPT OF PHYSICS, CAMPUS BOX 390  
BOULDER, CO 80309  
ATTN: DR A. LEVSHIN  
ATTN: DR. R. ENGDAHL  
ATTN: M. RITZWOLLER  
ATTN: PROF C. ARCHAMBEAU

COLUMBIA UNIVERSITY  
LAMONT - DOHERTY EARTH OBSERVATORY  
PALISADES, NY 10964  
ATTN: DR J. XIE  
ATTN: DR W. Y. KIM  
ATTN: PROF P.G. RICHARDS  
ATTN: DR. M. TOLSTOY

UNIVERSITY OF CONNECTICUT  
DEPARTMENT OF GEOLOGY & GEOPHYSICS  
STOORS, CT 06269 - 2045  
ATTN: PROF V.F. CORMIER, U -45,  
ROOM 207

CORNELL UNIVERSITY  
DEPARTMENT OF GEOLOGICAL SCIENCES  
3126 SNEE HALL  
ITHACA, NY 14853  
ATTN: PROF M.A. BARAZANGI

HARVARD UNIVERSITY  
HOFFMAN LABORATORY  
20 OXFORD STREET  
CAMBRIDGE, MA 02138  
ATTN: PROF A. DZIEWONSKI  
ATTN: PROF G. EKSTROM

INDIANA UNIVERSITY  
DEPARTMENT OF GEOLOGICAL SCIENCES  
1005 10TH STREET  
BLOOMINGTON, IN 47405  
ATTN: PROF G. PAVLIS

IRIS  
1200 NEW YORK AVENUE, NW SUITE 800  
WASHINGTON, DC 20005  
ATTN: DR D. SIMPSON  
ATTN: DR G.E. VAN DER VINK

IRIS  
1408 NE 45TH ST #201  
SEATTLE, WA 98105  
ATTN: DR. T. AHERN

MASSACHUSETTS INSITUTE OF TECHNOLOGY  
EARTH RESOURCES LABORATORY  
42 CARLETON STREET  
CAMBRIDGE, MA 02142  
ATTN: DR W. RODI  
ATTN: PROF M. N. TOKSOZ

MICHIGAN STATE UNIVERISTY LIBRARY  
450 ADMINISTRATION BUILDING  
EAST LANSING, MI 48824  
ATTN: K. FUJITA

NEW MEXICO STATE UNIVERSITY  
DEPARTMENT OF PHYSICS  
LAS CRUCES, NM 88003  
ATTN: PROF J. NI  
ATTN: PROF T. HEARN

NORTHWESTERN UNIVERSITY  
DEPARTMENT OF GEOLOGICAL SCIENCES  
1847 SHERIDAN RD  
EVANSTON, IL 60208  
ATTN: PROF E. OKAL

PENNSYLVANIA STATE UNIVERSITY  
GEOSCIENCES DEPARTMENT  
403 DEIKE BUILDING  
UNIVERSITY PARK, PA 16802  
ATTN: PROF C. AMMON  
ATTN: PROF S. ALEXANDER  
ATTN: DR. A. NYBLADE

SAN DIEGO STATE UNIVERSITY  
DEPARTMENT OF GEOLOGICAL SCIENCES  
SAN DIEGO, CA 92182  
ATTN: PROF S.M. DAY

DISTRIBUTION LIST  
DTRA - TR - 00 - 15

SOUTHERN METHODIST UNIVERSITY  
DEPARTMENT OF GEOLOGICAL SCIENCES  
P.O. BOX 750395  
DALLAS, TX 75275  
ATTN: B. STUMP  
ATTN: E. HERRIN  
ATTN: H.L. GRAY  
ATTN: P. GOLDEN

UNIVERSITY OF HAWAII - MANOA  
P.O. BOX 1599  
KAILUA - KONA, HI 96745 1599  
ATTN: DR. M. A. GARCES

UNIVERSITY OF MISSISSIPPI  
1 COLISEUM DRIVE  
UNIVERSITY, MS 38677  
ATTN: PROF. H. BASS

UNIVERSITY OF SOUTHERN CALIFORNIA  
520 SEASIDE SCIENCE CENTER  
UNIVERSITY PARK  
LOS ANGELES, CA 90089 - 0483  
ATTN: PROF C. G. SAMMIS  
ATTN: PROF T. JORDAN

WASHINGTON UNIVERSITY  
DEPARTMENT OF EARTH PLANET SCI  
ONE BROOKINGS DRIVE  
SAINT LOUIS, MO 63130 - 4899  
ATTN: DR. G. SMITH

UNIVERSITY OF WISCONSIN - MADISON  
1215 W DAYTON ST  
MADISON, WI 53706 - 1600  
ATTN: DR. C. THURBER

ST LOUIS UNIVERSITY  
P.O. BOX 8148  
PIERRE LACLEDE STATION  
ST LOUIS, MO 63156 - 8148  
ATTN: PROF B.J. MITCHELL  
ATTN: PROF R. HERRMAN

UNIVERSITY OF MEMPHIS  
3890 CENTRAL AVE  
MEMPHIS, TN 38152  
ATTN: DR. J. PUJOL  
ATTN: DR. C. LANGSTON

UNIVERSITY OF TEXAS - AUSTIN  
P.O. BOX 7726  
AUSTIN, TX 78712  
ATTN: DR. J. PULLIAM  
ATTN: DR. M. SEN

UNIVERSITY OF TEXAS - EL PASO  
DEPT OF GEOLOGICAL SCIENCES  
EL PASO, TX 79901  
ATTN: PROF G. KELLER  
ATTN: DR. D. DOSER  
ATTN: DR. A. VELASCO

FOREIGN

AUSTRALIAN GEOLOGICAL SURVEY  
ORGANIZATION  
CORNER OF JERRAGOMRRRA &  
NINDMARSH DRIVE  
CANBERRA, ACT 2609  
AUSTRALIA  
ATTN: D. JEPSON

GEOPHYSICAL INSTITUTE OF ISRAEL  
POB 183  
LOD, 71100 ISRAEL  
ATTN: DR Y. GITTERMAN  
ATTN: DR. A. SHAPIRA

GEOLOGICAL SURVEY OF CANADA  
7 OBSERVATORY CRESCENT  
OTTAWA K1A 0Y3 ONT  
CANADA  
ATTN: C. WOODGOLD

I.R.I.G.M. - B.P. 68  
38402 ST. MARTIN DE HERES  
CEDEX, FRANCE  
ATTN: DR M. BOUCHON

MINISTRY OF DEFENSE  
PROCUREMENT EXECUTIVE  
BLACKNESS, BRIMPTON  
READING RG7-4RS ENGLAND  
ATTN: DR. D. BOWERS

DISTRIBUTION LIST  
DTRA - TR - 00 - 15

NTNF/NORSAR  
P.O. BOX 51  
N- 2007 KJELLER, NORWAY  
ATTN :DR. F. RINGDAL  
ATTN: T. KVAERNA  
ATTN: S. MYKKELTVEIT

OBSERVATORIE DE GRENOBLE  
I.R.I.G.M. - B.P. 53  
38941 GRENOBLE, FRANCE  
ATTN: DR. M. CAMPILLO

OBSERVATORIO SAN CALIXTO  
INDABURO #944  
CASILLA 12656  
LA PAZ  
BOLIVIA  
ATTN: E. MINAYA

RESEARCH SCHOOL OF EARTH STUDIES  
INSTITUTE OF ADVANCED STUDIES  
G.P.O. BOX 4  
CANABERRA 2601, AUSTRALIA  
ATTN: PROF. B.L.N. KENNETT

PTS/CTBTO  
VIENNA INTERNATIONAL CIRCLE  
P.O. BOX 1200  
VIENNA A - 1400  
AUSTRIA  
ATTN: P. BASHAM  
ATTN: DR. P. FIRBAS  
ATTN: DR. R. KEBEASY

RHUR UNIVERSITY/BOCHUM  
INSTITUE FOR GEOPHYSIK  
P.O. BOX 102148  
463 BOCHUM 1, GERMANY  
ATTN: PROF H.P. HARJES

UNIVERSITY OF BERGEN  
INSTITUE FOR SOLID EARTH PHYSICS  
ALLEGATION 41  
N-5007 BERGEN, NORWAY  
ATTN: E. HUSEBYE

UNIVERSITY OF CAMBRIDGE  
DEPARTMENT OF EARTH SCIENCES  
MADINGLEY RISE, MADINGLEY ROAD  
CAMBRIDGE CB3 0EZ, ENGLAND  
ATTN: PROF K. PRIESTELY

DEPARTMENT OF DEFENSE CONTRACTORS

BATTELLE MEMORIAL INSTITUTE  
MUNTIONS & ORDANCE CTR  
505 KINGS AVENUE  
COLUMBUS, OH 43201 - 2693  
ATTN: TACTEC

BBN CORPORATION  
1300 N 17TH STREET, SUITE 1200  
ARLINGTON, VA 22209  
ATTN: DR. D. NORRIS  
ATTN: R. GIBSON  
ATTN: J. PULLI

CENTER FOR MONITORING RESEARCH  
1300 N 17TH STREET, SUITE 1450  
ARLINGTON, VA 22209 - 2402  
ATTN: DR. K. L. MCLAUGHLIN  
ATTN: DR. R. WOODSWARD  
ATTN: DR. R. NORTH  
ATTN: DR. V. RYABOY  
ATTN: DR. X. YANG  
ATTN: LIBARIAN  
ATTN: J. MURPHY  
ATTN: I. BONDAR  
ATTN: DR. B. KOHL

ENSCO INC  
P.O. BOX 1346  
SPRINGFIELD, VA 22151 - 0346  
ATTN: D. BAUMGARDT  
ATTN: Z. DER

ITT INDUSTRIES  
ITT SYSTEMS CORPORATION  
1680 TEXAS STREET SE  
KIRTLAND AFB, NM 87117 5669  
2 CYS    ATTN: DTRIAC

DISTRIBUTION LIST  
DTRA - TR - 00 - 15

MISSION RESEARCH CORPORATION  
8560 CINDERBED ROAD, SUITE 700  
NEWINGTON, VA 22122  
ATTN: DR M. FISK  
ATTN: R. BURLACU

MULTIMAX, INC  
1441 MCCORMICK DRIVE  
LANDOVER, MD 20785  
ATTN: DR. I. N. GUPTA  
ATTN: DR. W. CHAN  
ATTN: W. RIVERS

MULTIMAX INC  
1090 N HIGHWAY A1A SUITE D  
INDIALANTIC, FL 32903  
ATTN: DR. H. GHALIB

SCIENCE APPLICATIONS INT'L CORP  
10260 CAMPUS POINT DRIVE  
SAN DIEGO, CA 92121 - 1578  
ATTN: DR G. E. BAKER  
ATTN: DR J. STEVENS  
ATTN: DR D. ADAMS  
ATTN: DR M. ENEVA

SCIENCE APPLICATIONS INT'L CORP  
1227 S. PATRICK DR SUITE 110  
SATELLITE BEACH, FL 32937  
ATTN: DR M. FELIX  
ATTN: DR H. GIVEN

TITAN CORPORATION (ATS)  
1900 CAMPUS COMMONS DRIVE  
SUITE 600  
RESTON, VA 20191 - 1535  
ATTN: DR C. P. KNOWLES

URS CORPORATION  
566 EL DORADO STREET  
PASADENA, CA 91009 - 3245  
ATTN: DR B. B. WOODS  
ATTN: DR C. K. SAIKIA  
ATTN: DR G. ICHINOSE

WESTON GEOPHYSICAL CORPORATION  
57 BEDFORD ST, SUITE 102  
LEXINGTON, MA 02420  
ATTN: DR D REITER  
ATTN: J. LEWKOWICZ  
ATTN: DR A. ROSCA  
ATTN: DR I. TIBULEAC  
ATTN: M. JOHNSON

WESTON GEOPHYSICAL CORPORATION  
917 ELLIS AVE SUITE 222  
LUFKIN, TX 75904  
ATTN: DR J. BONNNER

WESTON GEOPHYSICAL CORPORATION  
411 NW 26TH ST  
GAINESVILLE, FL 32607  
ATTN: DR S. RUSSELL